PL-TR-93-3025
OCT 11 1993

PL-TR--
93-3025

SOLAR CONCENTRATOR SYSTEM DEVELOPMENT

Edward S. Kovacik

TRW Space and Electronics Group
One Space Park
Redondo Beach CA 90278

August 1993

Final Report

PHILLIPS LABORATORY
Propulsion Directorate
AIR FORCE MATERIEL COMMAND
EDWARDS AIR FORCE BASE CA 93524-7001

FOREWORD

This final technical report was prepared by TRW Space and Electronics Group, Redondo Beach CA under contract F046111−91−C−0043, for Operating Location AC, Phillips Laboratory, Edwards AFB CA 93524−7001. Project Manager for Phillips Laboratory was Kristi Laug.

This report represents the results of research study and design tasks which were performed over an extended period of performance. During that time many people contributed to the work accomplishment. In particular the author would like to acknowledge the technical support: Michael T. Izumi for preparing the computer aided design configuration layouts and drawings; and Abner Kaplan and Irvin S. Chan for performing the structural and thermal distortion analyses.

The report has been reviewed and is approved for release and distribution in accordance with the distribution statement on the cover and on the SF Form 298.

KRISTI K. LAUG
Project Manager

BERNARD R. BORNHORST
Chief, Space Propulsion Branch

LAWRENCE P. QUINN
Deputy Director
Applications Engineering Division

REPORT DOCUMENTATION PAGE

Form Approved
OMB No 0704–0188

Public reporting burden for this collection of information is estimated to average 1 hour per responce, including the time for reviewing instructions searching existing data sources gathering and maintaining the data needed, and completing and reviewing the collection of information. Send comments regarding this burden estimate or any other aspect of this collection of information, including suggestions for reducing this burden to Washington Headquarters Services, Directorate for Information Operations and Reports, 1215 Jefferson Davis Highway, Suite 1204, Arlington, VA 22202–4302, and to the Office of Management and Budget, Paperwork Reduction Project (0740–0188), Washington DC 20503.

1. AGENCY USE ONLY (LEAVE BLANK	2. REPORT DATE	3. REPORT TYPE AND DTAES COVERED
	August 1993	Final Report

4. TITLE AND SUBTITLE
SOLAR CONCENTRATOR SYSTEM DEVELOPMENT

5. FUNDING NUMBERS
C: F29601-91-C-0043
PE: 62302F
PR: 3058
TA: 00CS

6. AUTHOR(S)
Edward S. Kovalcik

7. PERFORMING ORGANIZATION NAME(S) AND ADDRESS(ES)
TRW Space and Electronics Group
One Space Park
Redondo Beach, CA 90278

8. PERFORMING ORGANIZATION REPORT NUMBER

9. SPONSORING/MONITORING AGENCY NAME(S) AND ADDRESS(ES)
Phillips Laboratory (AFMC)
OLAC PL/RKAS
Edwards AFB, CA
93523–5000

10. SPONSORING/MONITORING AGENCY REPORT NUMBER
PL–TR–93–3025

11. SUPPLEMENTARY NOTES

COSATI CODE(S):

12a. DISTRIBUTION/AVAILABILITY STATEMENT
Distribution authorized to U.S. Government agencies and their contractors; Critical Technology, August 1993. Other requests for this document must be referred to OLAC PL/TSR, 5 Pollux Ave. Edwards AFB, CA 93524–7015

12b. DISTRIBUTION CODE
C

13. ABSTRACT (MAXIMUM 200 WORDS) Extended abstract continued on next page

Solar thermal propulsion rockets have been under investigation as an efficient, reusable orbit transfer spacecraft stage. The propulsion system uses solar energy, which is collected by large mirror concentrators to heat hydrogen gas for expansion through propulsion nozzles. This paper summarizes work performed under Air Force Phillips Laboratory contract which investigated the integrating structure and gimbal arrangement for tracking the sun during propulsion systems mission performance. Conceptual designs were configured for structural interconnecting elements and gimbal actuation system in both the stowed launch and deployed on–orbit conditions. Structural member approaches investigated inflatable rigidized struts and deployable lattice truss booms. The recommended structural configuration uses six (6) inflatable rigidized struts to support the inflatable solar concentrator, and analytical results are presented for both structural dynamic and thermoelastic distortions under the missions environments. Analysis results are compared to system requirements, i.e., structural deployed deflection/stiffness/stability and thermal distortion/sun pointing accuracy. Further component and structure development, demonstration and overall system study is recommended in order to improve and validate the solar thermal propulsion concept.

14. SUBJECT TERMS
Solar Concentrators; Solar Thermal Propulsion; Solar Rocket Support; Structure and Gimbal; Structural Dynamic and Thermal Distortion Analysis

15. NUMBER OF PAGES

16. PRICE CODE

17. SECURITY CLASSIFICATION OF REPORT	18. SECURITY CLASSIFICATION OF THIS PAGE	19. SECURITY CLASSIFICATION OF ABSTRACT	20. LIMITATION OF ABSTRACT
Unclassified	Unclassified	Unclassified	SAR

NSN 7540–010280–5500

Standard Form 298 (Rev 2–89)
Prescribed by ANSI Std 239–18
298–102

ACKNOWLEDGMENTS

This report presents the results of research study and design tasks which were performed over an extended period of performance. During that time many people contributed to the work accomplishment. In particular, the technical support of the following people is acknowledged.

Computer aided design configuration layouts and drawings were prepared by Michael T. Izumi. Structural and thermal distortion analyses were performed by Abner Kaplan and Irvin S. Chan.

Finally, grateful acknowledgment is made for Air Force Phillips Laboratory Contract Program Manager Kristi K. Laug, who provided monitoring guidance and allocation of resources to support the performance of the contract.

TABLE OF CONTENTS

LIST OF FIGURES

LIST OF TABLES

INTRODUCTION

This report is the Final Technical Report under Contract F29601-91-C-0043. The report incorporates results of the entire contract performance from its inception through completion, and includes all available data generated under the contract.

The contract objectives are to study and analyze conceptual designs for the supporting structure and gimbal actuation system for a solar thermal propulsion spacecraft stage. The propulsion system is intended as a reusable orbit transfer vehicle which would dock with large payloads and propel them from low earth orbit to higher orbits and/or interplanetary missions. The propulsion system uses solar energy, which is collected by large mirror concentrators to heat gas working fluid and produce the propulsive thrust by expanding the heated gas through a rocket nozzle. The estimated specific impulse of the solar thermal propulsion rocket is approximately 1000 lbf of rocket thrust produced by each lbm of hydrogen propellant expelled during each second of time. In order to develop this level of propulsion performance, the hydrogen gas must be heated to approximately 5000°R using concentrated solar energy. This propulsion performance is based upon previous Air Force contracts and other studies (References 1 through 5) which have investigated the solar propulsion system and individual components. Reference 6 summarizes the solar propulsion concept and background, and it was used in the present contract study as the basis for design of the supporting structure/gimbal system. Figure 1 (Reference 2) depicts the solar thermal propulsion concept configuration. Payloads of up to 30,000 lb can be transferred to geosynchronous orbit using a 20,000 lb propulsion stage. The propulsion stage consists of a large tank containing hydrogen propellant and two large diameter offset paraboloidal mirrors, which concentrate solar energy into thruster cavities. The cavities act as heat exchangers to heat the hydrogen gas for expansion through dual rocket nozzles, producing approximately 40 lb of thrust each.

The present contract investigated the integrating structure and the gimbal arrangement for tracking the sun during mission performance. The study was organized into four main tasks: 1) Define structure arrangements and materials which meet the solar thermal propulsion system requirements; 2) Identify gimbal actuation concepts which meet motion and sun pointing requirements; 3) Conduct structural dynamic and thermal distortion analysis of the supporting structural arrangement; 4) Prepare concept layout drawings, and report the study results in a final technical report.

SUMMARY

Conceptual designs were configured for structural elements and gimbal actuation system to support large solar concentrators for a solar thermal propulsion spacecraft. Structural design requirements are based upon compatibility with components and overall system performance as defined by previous and on-going Air Force research studies.

In order to select a recommended structural approach, preliminary configuration layouts and simplified analyses were conducted for several structural concepts, including inflatable rigidized struts and deployable lattice truss booms. Based upon these design studies, the following structural system is recommended.

- A large diameter multiple discrete follower roller bearing gimbal, based upon development work for the Space Station Solar Alpha Rotary Joint.

- Six (6) inflatable/rigidized struts arranged as three bipod sets to support the inflatable concentrator.

- Support struts and torus acting as a combined structural system with structural modulus of 500,000 psi and low coefficient of thermal expansion (CTE) similar to Kevlar composite.

This structural arrangement was analyzed to establish the following structural characteristics.

- Steady-state thrust induced acceleration causes low levels of stress and surface distortion (2.2 mrad maximum slope error).

- Structural dynamic fundamental frequency is greater than 0.1 Hz (0.17 Hz) which is generally acceptable for large spacecraft appendages.

- Structural dynamic mode shapes are favorable for the solar concentration function; in that, the first two modes result in only sun pointing type errors, with lower distortion higher modes affecting the concentrator surface shape (precision) modes.

- Gimbal bearing stiffnesses similar to those being developed for the Space Station Alpha Joint are more than adequate for solar propulsion.

- Thermoelastic characteristics, which are controlled by the low CTE struts and torus, cause low stress and thermal distortion. However, the high CTE polymer inflatable concentrator materials show large distortions.

Finally, although many simplifying assumptions have been made, the study indicates a viable structural and gimbal arrangement. Most concerns for this structural concept are related to the inflatable concentrator in meeting surface shape and structural requirements, i.e., deployed shape, stiffness, stability, and thermal distortion. The inflatable elements are the key to viable solar thermal propulsion, and further development and demonstration is needed. Also, inflatable concentrator limitations may be helped by reassessing overall system configurations and mission thrust profile trades, including thermal storage, in order to consider other focusing systems (axisymmetric, secondary reflectors, active optics, etc.) which might alleviate surface shape precision requirements for the inflatable concept.

RESEARCH PERFORMED

The following sections describe the design studies that were performed during the contract period.

Solar Propulsion System Components and Configuration

Figures 1 and 2 show the overall solar thermal rocket configuration. As presented in Reference 6, it consists of the following major elements:

- Two offset parabolic mirror concentrators 100 ft. projected diameter
- Concentrator focal length 49 ft
- Concentrators are inflatable deployed
- Concentrator structural interface at peripheral inflatable torus
- Propulsion stage weight 20,000 lb maximum
- Payload weight 30,000 lb maximum for LEO to GEO
- Gimbal sun tracking 2-axis, all angles
- Thruster cavity diameter 1.0 ft (10,000 to 1 area concentration ratio)
- Preliminary structural design load, 0.008g any direction

The present study is concerned with the conceptual design of the interconnecting structural members and gimbal as related to the solar concentrator sun tracking and energy focusing functions. The support structure must interface with various system components and be compatible with the inflatable deployment of the concentrator and torus. The key components which were incorporated into the structure design study are listed in Table 1, and they will be described briefly in the following sections.

Concentrator/Torus. Inflatable structures are used for the large solar concentrators because they are lightweight, self-deployable and package very efficiently for launch. These factors allow the solar propulsion concept to be feasible as an efficient and high performance propulsion concept. The concentrator and torus are made of thin film polymers which are inflated in orbit by a low pressure gas. The parabolic portion of the concentrator uses a thin vacuum deposited aluminum coating on the polymer as the solar mirror surface. The enclosing canopy is a solar transparent thin film to provide the concentrator inflatable enclosure. The torus is a separate pressurized enclosure made of thin polymer materials. Several different approaches have been investigated (References 4, 5, 7) to obtain and retain the final on-orbit shape, as listed below.

- Pressure stabilized by life gas supply
- Inflated and chemically rigidized
- Combination of the two above approaches

For the present structure design study, the concentrator was assumed to be pressure stabilized by a low pressure gas supply over its entire life, and the supporting torus was assumed to be inflated and then chemically rigidized. Thus in the structural analysis, the torus structural parameters could be optimized in conjunction with the support strut system. Gas inflation process is depicted in Figure 3 (Reference 7) for a concentrator/torus.

Support Struts. In conjunction with the inflatable concentrator/torus development, discussed above, inflatable tubular struts have also been investigated (References 4 and 5). In addition to pressure stabilized and chemically rigidized struts, foam-in-place and thin aluminum foil tubes have been considered. Again, for the present structure design study, chemically rigidized tubes were assumed for the interconnecting strut system.

Deployable Lattice Truss. In addition to the inflatable and rigidized struts described above, articulated longeron deployable booms were also considered as interconnecting structure components. This type of spacecraft structure is highly developed (see Figure 4, Reference 8) and can be constructed from graphite composite material which has high rigidity and very low thermal distortion. Deployment is motorized from a canister container, as shown in Figure 5 (Reference 9). Three and four longeron booms already have been developed and flown.

Solar Cavity/Thruster. Each solar concentrator has a cavity type heat exchanger located at the focal point. The cavity opening is 12 inches in diameter, see Figure 6 (References 3 and 10). The solar energy enters the cavity and is absorbed by a tubular heat exchanger, which heats the hydrogen propellant gas flowing in the tubes. Other heat exchange approaches, such as porous carbon foam or particulate mixing, have also been considered (References 1 and 11). The heated hydrogen is expanded through a small rocket nozzle to provide propulsion thrust. The cavity and thruster must be fabricated from materials which can withstand the high solar flux and gas temperatures. Extensive thermal insulation and isolation must be utilized to prevent heat loss and to protect lower temperature components and structure.

Gimbal Bearing System. Obviously, for the large diameter solar concentrators and long length support struts, a large diameter gimbal bearing is required. Extensive development has been conducted for the Space Station Solar Alpha Rotary Joint bearing system (Reference 12). The bearing design is shown in Figure 7, and it has been adopted for the present study because of its high stiffness characteristics and its advanced development status. The bearing is 120 inches in diameter, and it consists of a stationary 120 inch diameter continuous race and a matching rotating race. Multiple discrete follower roller bearing packages provide the bearing rotation between races. The races are supported by cylindrical thin wall skirts which allow for thermal expansion. Reference 12 presents bearing stiffness characteristics for both the 120 inch and 64 inch diameter bearing systems which will be used in the present study analyses for comparison. The bearing provides only one axis of rotation for tracking the sun. It is assumed that the other axis of rotation is obtained by rolling the entire vehicle (including propellant tank and payload) about the tank axis using a separate attitude control system. An alternate would be to incorporate a large diameter bearing at the tank interface in order to provide a beta axis gimbal. But this would complicate the transfer of hydrogen propellant from the stationary tank to the gimbaled cavity thrusters.

Propellant Tank and Payload. These components of the solar thermal rocket are not part of the present study tasks, but they are shown in configuration layouts to demonstrate compatibility and depict the overall concept.

Structural Concept Description

Structural concept layouts were prepared for stowed launch packaging and deployed configurations for several structural approaches, as listed below and depicted in Figure 8.

- Six (6) inflatable/rigidized struts in bipod arrangement
- Three (3) inflatable/rigidized struts (four struts were also considered)
- Deployable lattice truss booms and guy-lines

Simplified static structural analysis was conducted for each case in order to identify the concept with the smallest static deflections. For each concept the 120 inch gimbal bearing diameter was used with the heat exchanger cavity located at the concentrator focus. In each case, a container was configured to house the stowed inflatable components, and a deployment sequence was established. Folded concentrator and strut packaging volume is based upon Reference 7, which limits double fold creasing.

Six (6) Inflatable/Rigidized Struts. Figure 9 shows the deployed six strut configuration. The structural arrangement consists of pairs of struts(bipods) which support the concentrator torus at equally spaced locations. Each strut line of action extends through the section modulus center of the torus and the 120 inch diameter bearing races. The stowed configuration is shown in Figure 10. The entire stowed vehicle fits within the 15 foot diameter Shuttle or Titan 4 launch envelope. The stowed inflatable components are enclosed in a segmented container for launch. At the time of deployment, the segments open to release the inflatable elements. The deployment sequence is as follows.

1. Open container segments
2. Inflate struts to deploy concentrator/torus
3. Fully inflate torus, concentrator and struts
4. Chemically rigidized struts and torus

In the deployed configuration the segmented container might be designed to automatically close, so as to provide a solar shield to protect low temperature components from concentrated solar energy during off-axis sun conditions or perhaps to modulate solar power during heat-up conditions. For clarity, thermal insulation materials are not shown, but they would be critical in order to meet thermal performance and safety requirements. Figure 11 shows the modularity of the solar propulsion vehicle. Only the concentrator, thruster and gimbal package is the subject of the present contract study.

Three (3) Inflatable/Rigidized Struts. Figure 12 shows the deployed three strut configurations. The struts are equally spaced at the 120 inch diameter bearing and at the deployed concentrator torus. Four equally spaced struts were also evaluated in the structural analysis for comparison. Stowed packaging and deployment would be similar to the six strut concept previously discussed.

Deployable Lattice Truss Boom. Figure 13 shows a structural arrangement which uses canister deployed articulated longeron booms. The stowed configuration is shown in Figure 14. The stowed inflatable concentrator and torus are enclosed in a single container which is attached to two separate boom canisters, with one canister hinged to the gimbal bearing system. Release devices restrain the container and canisters during launch. The deployment sequence is as follows:

1. Release launch tie-downs
2. Rotate concentrator package and lock at proper angle
3. Deploy lower boom from canister and guy-lines from spools
4. Deploy upper boom from canisters and guy-lines from spools
5. Release concentrator/torus from container
6. Inflate concentrator and torus
7. Chemically rigidized torus
8. Adjust guy-line tensions to align concentrator

For structural analysis, it was assumed that the boom and guy-lines are graphite materials.

Structural Analysis

Analytical investigations were performed in several stages, from simplified classical curved beam analysis to Nastran finite element modeling. Preliminary simplified structural analysis was performed on the concentrator rim support torus as a separate structural member with varying number of support points. These results were used to "size" the torus and establish material property requirements. Then, the torus and support strut configurations, which were described in the previous sections, were analyzed for static load deflections using the COSMOS/M computer program. Finally, based upon these simplified analyses, the six strut bipod configuration was selected for NASTRAN analysis of structural dynamics and thermal distortion characteristics.

Torus Ring Analysis. A preliminary simplified parametric analysis of the rim support torus was performed to determine deformation and stress behavior under inertia loads as a function of the number of support points and other parameters. The elliptical torus was approximated as a circular toroid subjected to uniform transverse load and supported at uniformly spaced points. This allowed the use of equations for laterally loaded classical curved beams from Roark (Reference 13). Solutions were obtained by using the TK Solver computer program. It should be noted that this approximation of the elliptical torus by a circular torus was used only to investigate preliminary configurations of structural members which display low distortion characteristics. Subsequent finite element analysis of the elliptical torus and struts will be presented in the next section.

The circular torus radius was assumed as 61 feet (732 inches) approximately the average radius for the elliptical offset concentrator. The uniformly distributed lateral load is based upon total concentrator weight and 0.008 g load (Reference 4). Table 2 shows the maximum torus deflections at mid span between support points, and the torus bending stresses (σ_b) due to inertia loads. Also shown are the compressive stresses (σ_{MP})due to concentrator inflation pressure of 0.00025 psi (Reference 4). These are calculated stresses in the torus, and they can be compared to allowable local buckling strength (σ_{CR}) as approximated by the equation for buckling of an isotropic cylinder (Reference 14). Torus weight (W_T) is also shown. Based upon the previous studies (References 1 through 6), the following general requirements are assumed for sizing the torus.

- Deflection less than 1.5 inches (2 mrad slope error equivalent)
- Torus weight approximately 200 lbs. maximum
- Local allowable buckling strength (σ_{CR}) must be greater than calculated stresses in the torus (σ_b and σ_{MP})

From Table 2, it is seen that small deflections can be obtained with 3 and 4 support points and larger torus radii (r). However, local buckling allowable strength is low and exceeded by membrane pressure stresses in all cases. This indicates that higher modulus material (Kevlar) must be used.

Table 3 shows the results for three point support using higher modulus material (E = 500,000 psi). Table 3 indicates that even with the increase in material modulus, a tube wall thickness of 0.02 will not provide sufficient buckling strength. However, a tube with 0.03 inch wall thickness and a radius of 4 inches will provide a structural buckling safety factor of 1.3 (1210/907), a maximum deflection of 0.81 inches and a weight of 204 lbs; while a .04 thick tube with a radius of 3 inches will provide a structural factor of safety of 2.7 (2493/925), a maximum deflection of 1.44 inches and the same weight. The high structural margin is desirable because the actual buckling stress may be significantly lower than the computed value.

Based upon the preliminary simplified analysis, the following conclusions are established and carried into the more detailed analyses.

1. The inertia bending stresses are negligible compared to the stresses caused by concentrator membrane pressure reactions.

2. A cantilever support (n=1) requires at least two and preferably more guy wires to prevent large deflections.

3. The rim weight is a critical function of its modulus and requires a modulus of 500,000 psi to achieve a weight of about 200 lbs.

4. Based on these results, a modulus of 500,000 psi, thickness of 0.04 inch, and a diameter of 6 inches was assumed for the torus. The same values of modulus and thickness was assumed for the support columns.

5. Although local buckling has a reasonable factor of safety, concern is felt about the stability of the torus against global buckling. In principal, the rim torus is supported by the stiffness of the pressured membrane against both in-plane and out-of-plane buckling, but the effective value of this stiffness is unknown.

Configuration Static Load Analysis. Each of the basic support configurations, previously discussed, were mathematically modeled and analyzed using a finite element model and the COSMOS/M computer program. Table 4 presents the structural characteristics used in the analysis, and Figures 15A through 15D show the model geometries.

Analytic results are summarized in Table 5. Maximum deflections and member rotations are shown for both lateral and axial load directions under 0.008 g acceleration. Several different support strut diameters were investigated for each configuration. It is seen that, for the 3 and 4 strut arrangements, the deflections are quite large (21.7 to 72.9 inches). The deployable boom/guy wire case has good stiffness except for lateral loads due to low torsional stiffness of the single boom element even using a reinforced boom. It is seen that acceptable deflections (1.80 inches, 0.127 degrees rotation = 2.2 mrad) are obtained for the 6 strut bipod case; and, therefore, this configuration is used in the structural dynamic and thermal distortion analyses.

Structural Dynamic Analysis. Based upon the preliminary analysis results, the structure selected for final analysis consists of a reflective membrane, a canopy, an elliptical torus and three bipods. The membrane and the canopy are joined together by the torus to form an elliptical pillow-like configuration. The torus is pin joined to the bipods at 3 points. The structure is simply supported on the perimeter of a 120-inch diameter alpha joint-type bearing to form a rigid framework. The elliptical torus has a minor diameter of 1200 inches and a major diameter of 1634 inches. The reflective membrane has a focal length of 588.5 inches. The membrane and the canopy are inflated with pressure to maintain the paraboloidal shape. Reference 4 predicted that, for a similar size concentrator, an internal pressure of 0.00025 psi is required to maintain the paraboloidal surface accurately and free of wrinkles. Membrane and canopy under such a pressure will have a maximum tensile stress of 1625 psi. The stresses are then reacted by internal forces and moments in the torus, resulting in a nominal compressive force of 645 lbs preload in the torus.

The membrane and the canopy are made of 1/4 mil thick polymer or Teflon material with an assumed modulus of 100,000 psi. The torus and bipod are made of Kevlar cloth material with a cross section of 6-inch diameter by 0.04 inch thick wall. The laminate property for both the torus and the bipod are assumed to be 500,000 psi. The overall weight of the structure is 444 lbs. The material properties and weight breakdown used in the analysis are tabulated in Table 6.

The math model for the structure was developed by converting the COSMOS/M program to NASTRAN. The NASTRAN FEM consist of plate and bar elements as shown in Figure 16. The model has 366 grids with 1260 static degrees of freedom and 117 dynamic degrees of freedom. 688 triangular plate elements are used to model the membrane and the canopy. The torus and the bipods are modeled with 42 bar elements. The 120-inch diameter bearing to support the structure is modeled using spring elements. Stiffness values predicted in Reference 12 for both 64 and 120 inch bearings were used for comparison in the dynamic analysis. For reference these values are tabulated in Table 7.

Several analyses approaches were considered in performing the dynamic computations. Rigorous analysis should consider the non-linearities of the internally pressurized concentrator, and the complex analytical solutions required by the differential stiffness matrix of Reference 15 for compatibility of stress, forces and moments between the concentrator and torus. However, for the present conceptual design study, several simplifying assumptions were made. A uniform compressive force (645 lbs) was assumed for preload in the torus. This approximates the interaction of the concentrator and torus. Also, modes and frequencies were performed for the concentrator structure without the membrane and canopy. A reasonable approach was to assume that the membrane and the canopy are massless and the effects of masses are distributed around the torus.

Dynamic analysis was performed using the 120-inch diameter bearing to support the concentrator structure. Stiffness values for both the 64 and 120-inch bearings were used in the analysis without changing the dimensions of the bearing. Modes were identified and frequencies were computed for the models with and without the 645 lbs preload in the torus. The results for both bearing models without preload are tabulated in Table 8. Mode shapes for the 120-inch bearing model are presented in Figure 17 thru 23. The results for the smaller bearing with torus preload are presented in Table

9. The frequency for the structure with the preload is about 40% higher than the structure without the preload.

Based upon the structural dynamic analysis results, the following general conclusions are summarized.

1. From Tables 7 and 8, gimbal bearing stiffness decreases of 50% to 80% do not have a significant effect on frequency (0.173 Hz vs. 0.1728 first mode). This indicates that a lighter weight (lower stiffness) bearing can be considered.

2. From Tables 8 and 9, torus preload has a significant (40%) stiffening effect on the structure (0.1728 Hz vs. 0.2441 Hz). This may indicate that more recent concentrator concepts which do not have a toroidal stiffening ring (Reference 16 Single Chamber Concentrator) could require more substantial support strut systems to control structural dynamics. On the other hand, without the mass of the toroidal ring in the single chamber concept, the fundamental frequency should tend to increase.

3. From Figures 17 and 18, mode shapes for modes 1 and 2 are primarily sun point errors. Higher modes (Figures 19 thru 23), include concentrator surface distortions. However, if higher modes are excited, generally deflections should be smaller in higher modes. Also, gas pressure effects should cause high damping, and thus limit deflections and sun focusing degradation.

Thermal Distortion Analysis. Thermal distortion analyses were performed on the complete NASTRAN math model including plate elements to represent the inflatable membrane and canopy. The thermal distortion analysis was performed with and without preload in the torus for comparison of the effects of preload. The assumed temperature profile is shown in Figure 24. These temperatures are approximations based upon calculations of Reference 17 for the equilibrium temperatures of uniform, spherical, solar-absorbing gas inflated balloons, and Reference 18 which shows transient temperature characteristics for a sun facing concentrator and torus in low earth orbit. A steady state case was selected for analysis since thermal distortions are only critical in the full sun portion of orbit where propulsive thrust is generated. The coefficient of thermal expansion (CTE) was assumed to be 50.0×10^{-6} in/in/°F for the reflector membrane and the transparent canopy, and 1.7×10^{-6} in/in/°F for the torus and the bipod Kevlar material.

Computed maximum thermal stresses and distortions are summarized in Table 10. These stresses represent changes in membrane stress and would be superimposed on the stress due to pressurization (approximately 1600 psi). It is seen that the stresses are low in comparison with the material yield stress of 5000 psi for polymers.

Figure 25 shows the thermal distortion contour plot of the reflective membrane with 645 lbs preload in the torus. It is seen that the distortion at the rim torus is small (0.154 inches) due to the selection of low CTE material (Kevlar) for the torus and strut structural members. However, the high CTE reflector membrane shows a much larger distortion (6.5 inches maximum) and approximately 80 mrad maximum slope error between contour lines 1 and 2 near the torus at the top as shown in the figure. Perhaps these larger distortions can be corrected using inflation pressurization adjustments with a reflector surface precision sensor control system.

Based upon the thermal distortion analysis results, the following general conclusions are summarized.

1. Thermal stresses are low compared to stresses due to internal pressure.

2. Thermal effects on reflector surface distortions are significant; however, distortion is minimized by pre-stressing.

3. The selection of rigidized Kevlar for the torus and struts limits the thermal distortion at the boundaries of the reflector and canopy due to the low CTE, even with large thermal gradients in these members. Obviously, a lower CTE for the reflector membrane and canopy is preferred--if this is possible in thin film materials.

CONCLUSIONS AND RECOMMENDATIONS

Conclusions based upon the studies and research performed on this contract have been listed throughout the report, and they will be summarized in the following paragraphs along with associated recommendations.

It is concluded that a viable structural and gimbal approach consists of six (6) inflatable/rigidized struts and torus supporting the pressure inflated solar concentrator. This structural arrangement is attached to a discrete follower gimbal bearing similar to the Space Station Solar Alpha Rotary Joint. Analysis shows that the struts and torus must have structural properties similar to Kevlar composite, and it is recommended that industry contractors, who specialize in inflatables, continue development and space qualification of structurally adequate inflation and rigidization materials and processes.

Although local buckling of inflatable rigidized members show reasonable factors of safety, concern is felt about the unknowns of global buckling. Analysis and test verification is required to understand the overall buckling characteristics of these large thin wall structures, including nonlinear membrane/torus stress interactions.

Static and structural dynamic analysis results show that deflections and surface distortions are small for reasonable weight structures, and that dynamic frequencies are as expected for spacecraft appendages. However, the analysis should be expanded to include more detailed modeling, damping, and nonlinearities of the inflated solar concentrator and canopy.

Thermoelastic analysis results show that a CTE similar to Kevlar (1.7×10^{-6} in/in/°F) is required to control thermal distortions. Polymer thin films used for inflatable solar concentrators will have larger thermal distortions, and active shape control may be required. Alternate materials and system configurations should be considered to improve solar concentration.

Finally, as discussed above, the inflatable elements are the key to viable solar thermal propulsion, and further development and demonstration is needed. The unknowns and limitations of an inflatable solar concentrator may be helped by reassessing overall system configurations and mission thrust profile trades, including thermal storage, in order to consider other focusing systems (axisymmetric, secondary reflectors, active optics, etc.) which might alleviate surface shape precision requirements for the inflatable concept.

REFERENCES

1. Etheridge, F. G., "Solar Rocket System Concept Analysis," AFRPL-TR-79-79, under contract F04611-79-C-007, Rockwell International, Satellite Systems Division, Space Systems Group, December 1979.

2. Shoji, J. M., Frye P.E., "Solar Thermal Propulsion for Orbit Transfer," AIAA/ASME/SAE/ASEE 24th Joint Propulsion Conference, Boston, MA, AIAA-88-3171, July 1988.

3. Shoji, J. M., "Solar Rocket Component Study, AFRPL-TR-84-057, under contract F04611-80-C-0039, Rockwell International, Rocketdyne Division, February 1985.

4. Veal, G.R., "Highly Accurate Inflatable Reflectors, Phase II," AFRPL-TR-86-089, L'Garde, Inc., Tustin, CA, contract F04611-84-C-0054, March 1987.

5. Bradford, Rodney, "Research and Development of Large, Highly Accurate, Inflatable Reflectors," AFRPL-TR-86-074, Spectra Research Systems Technologies, contract F04611-84-C-0053, February 1987.

6. Laug, Kristi K., "The Solar Propulsion Concept is Alive and Well at the Astronautics Laboratory," 1989, JANNAF Propulsion Meeting, Cleveland, Ohio, CPIA Publication 515, Vol. I, pp. 289-324, May 1989.

7. Bernasconi, M. C., Pagana, E., Reibaldi, G. G., "Large Inflatable Space Rigidized Antenna Reflectors," IAF-87-315, 38th IAF Conference, Brighton U.K., October 1987.

8. Astro Aerospace Corporation, Technical Brochure, Carpinteria, CA

9. AEC-Able Engineering Company, Inc., Technical Brochure, Goleta, CA.

10. Frye, P. E., Shoji, J. M., Pard, A. G., "Solar Rocket Thruster Studies," PL-TR-91-3082, Rockwell International, Rocketdyne Division, July 1992.

11. Tuffias, Robert H., DelaRosa, Mark J., Kaplan, Richard B., "Advanced Materials for Solar-Thermal Propulsion," Ultramet, Pacoima, CA, ASME Solar Engineering-Vol. 2, pg 783, 1992

12. Everman, M. R., Jones, P. A., Spencer, P. A.,"Space Station Alpha Joint Bearing," 21st Aerospace Mechanisms Symposium, Houston, Texas, April 1987.

13. Young, W. C., "Roark's Formulas for Stress and Strain," McGraw-Hill Book Company, Sixth Edition, 1989.

REFERENCES (continued)

14. "Buckling of Thin-Walled Circular Cylinder," NASA SP-8007, August 1968.

15. Grossman, Gershon, "Analysis of Rim Supports for Off-Axis Inflatable Reflectors I, Loads," Journal of Aerospace Engineering, Vol. 4, No. 1, January 1991.

16. Gierow, Paul A, Clayton, William R, Kromis, Deborah, "Concentrator Technology," PL-TR-92-3030, SRS Technologies, Huntsville, AL, September 1992.

17. Thomas, M., Friese, G. J., "Pressurized Antennas for Space Radar," AIAA Publication CP807, December 1980.

18. Kovalcik, E. S., Castle, C. H., "Development Status of Aluminum Solar Concentrators," Third Biennial Aerospace Power Systems Conference, Philadelphia, PA, AIAA Paper 64-731, September 1964.

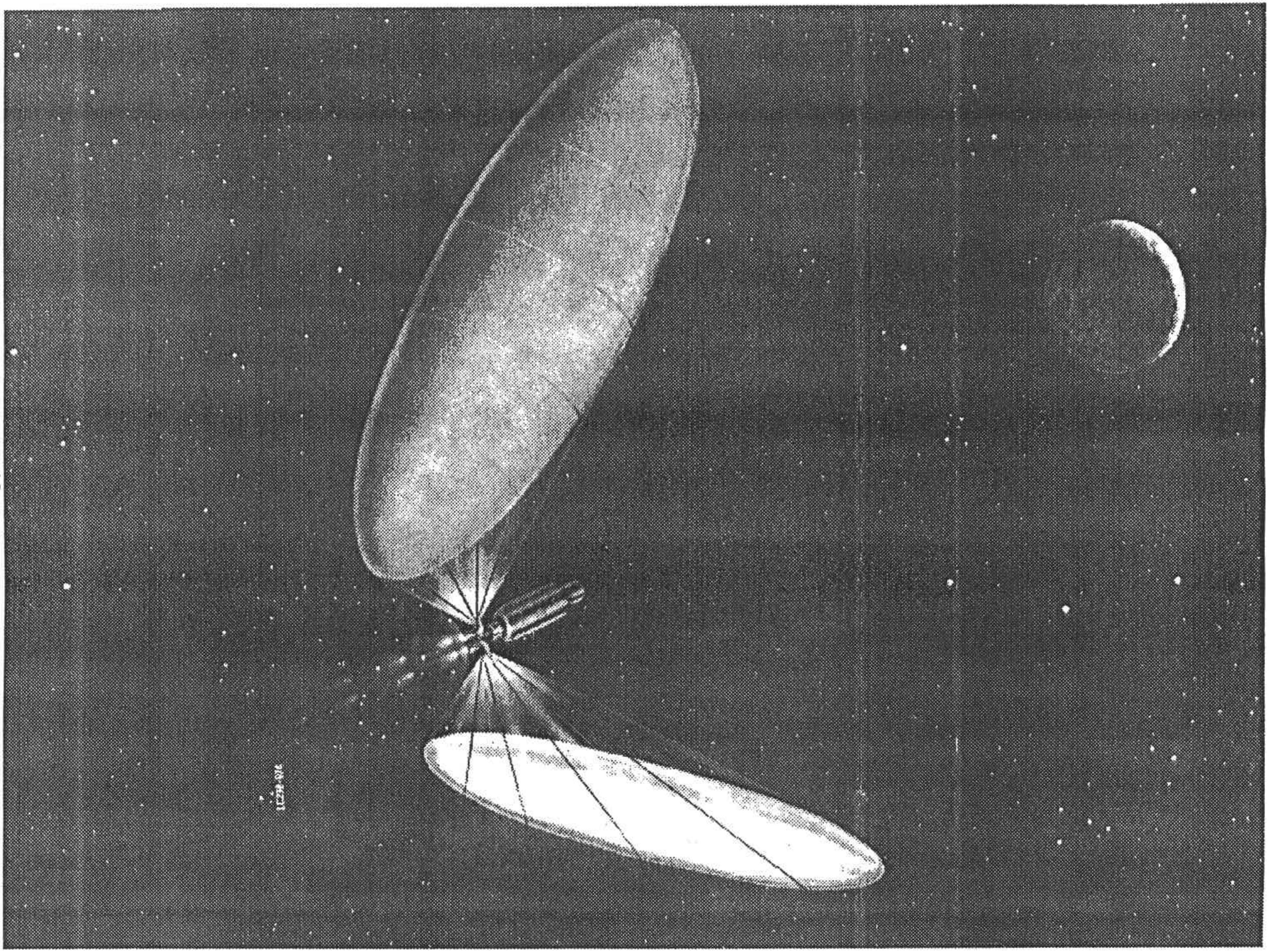

Figure 1. Solar Thermal Propulsion Concept (Reference 2)

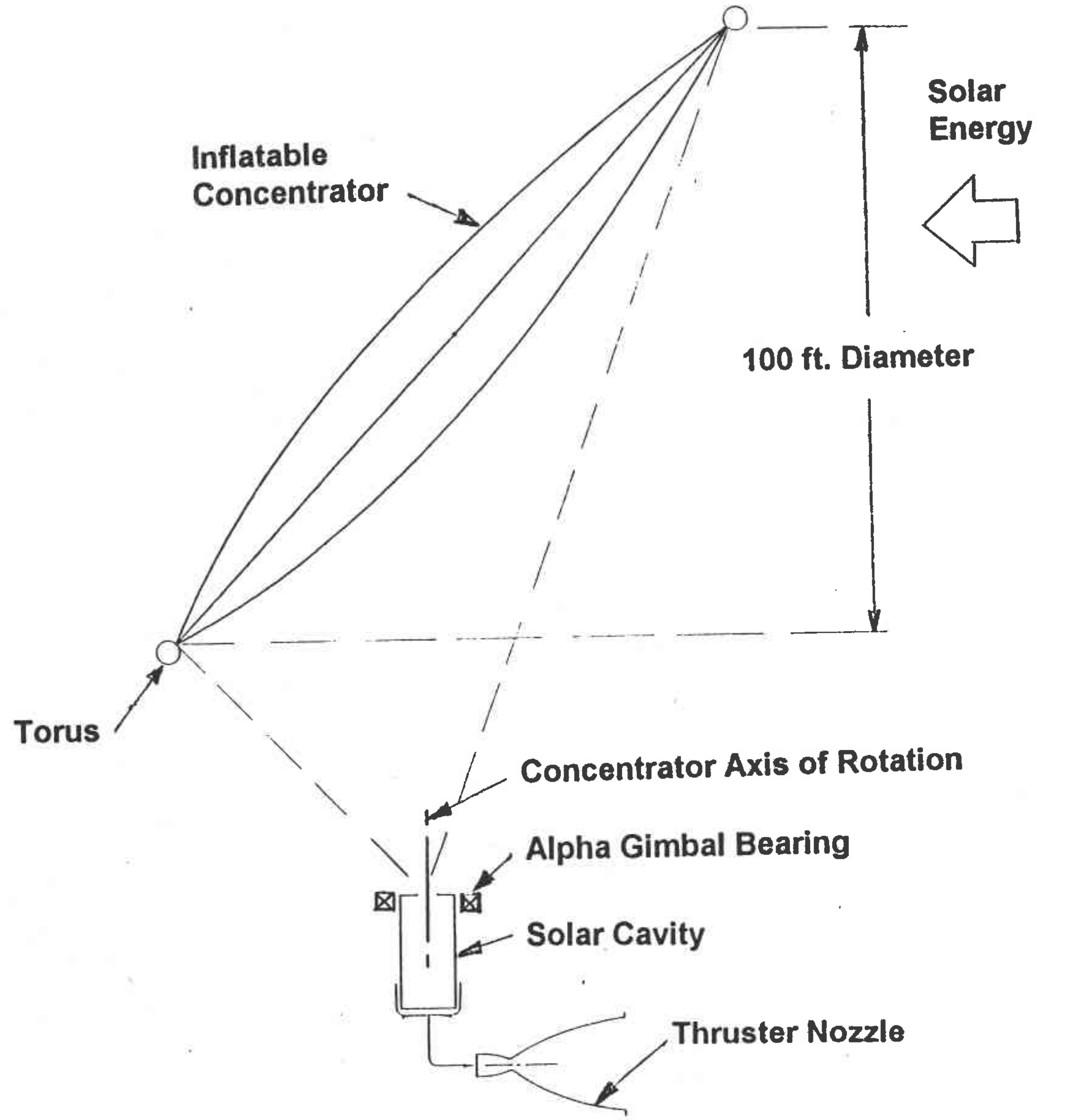

Figure 2. Solar Thermal Propulsion Concentrator/Thruster

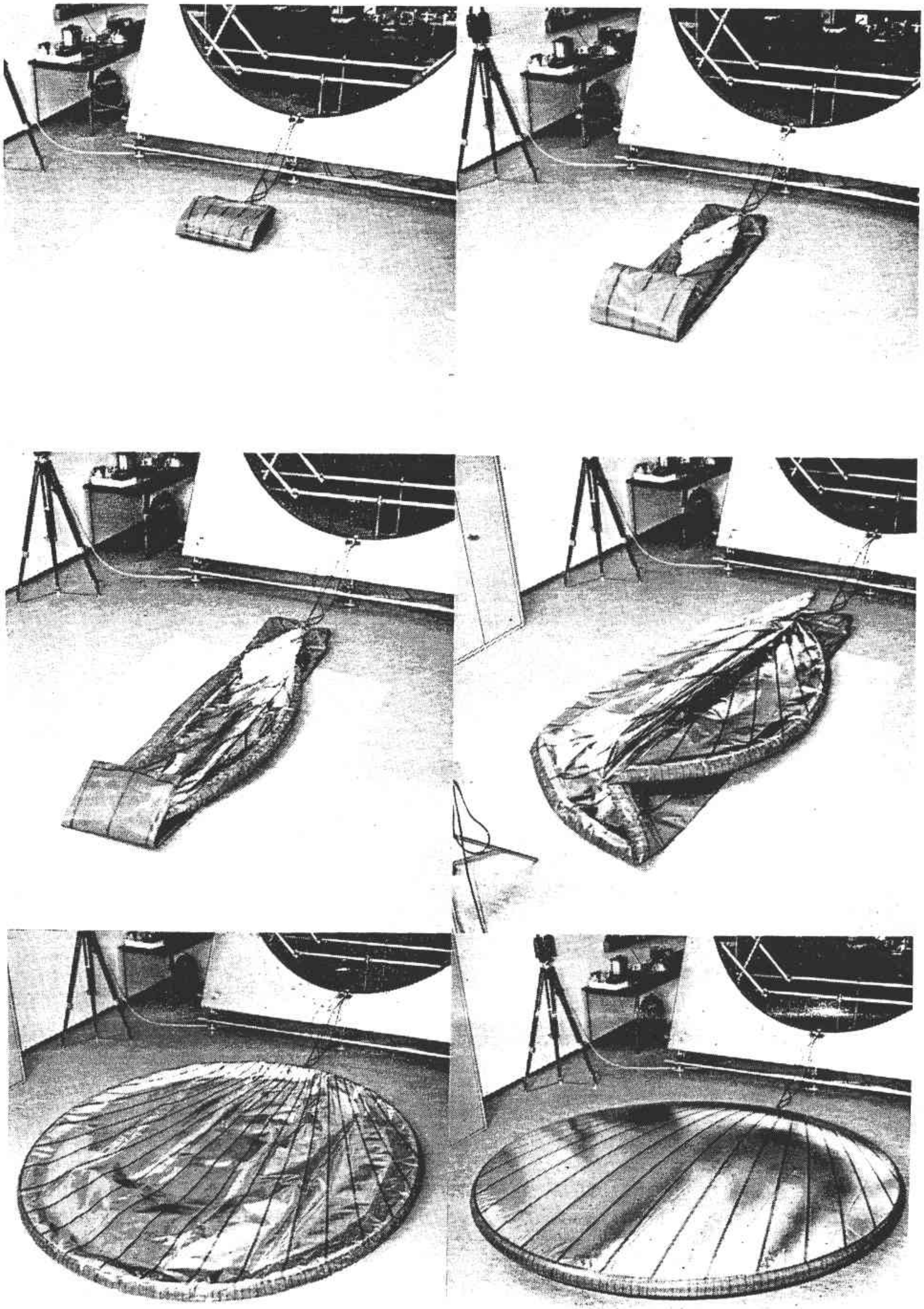

Figure 3. Concentrator/Torus Inflation (Reference 7)

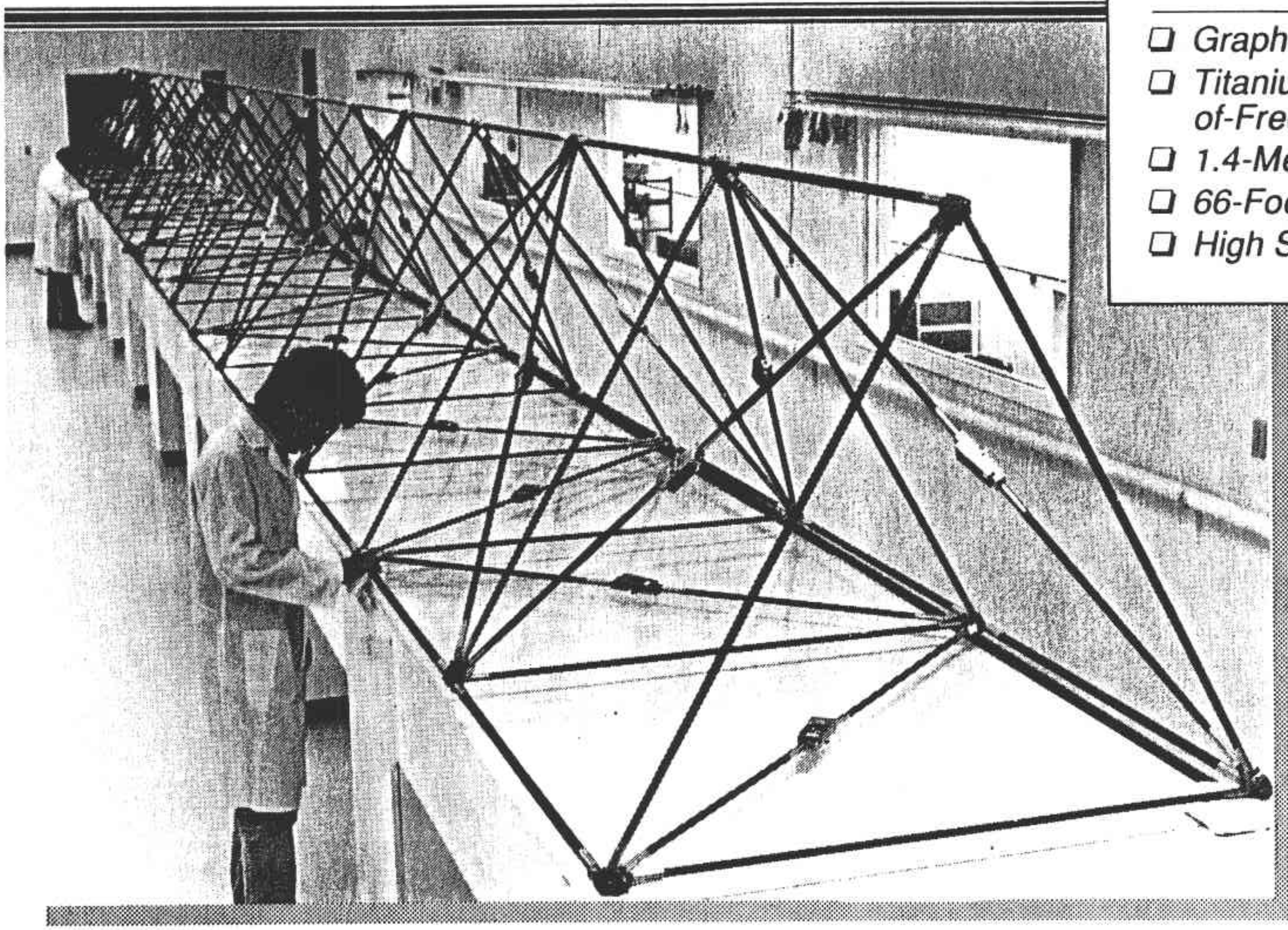

FEATURES

- Graphite/Epoxy Struts
- Titanium Single Degree-of-Freedom Hinges
- 1.4-Meter-Diameter
- 66-Foot Length
- High Stiffness

Figure 4. Articulated Longeron Lattice Truss (Reference 8)

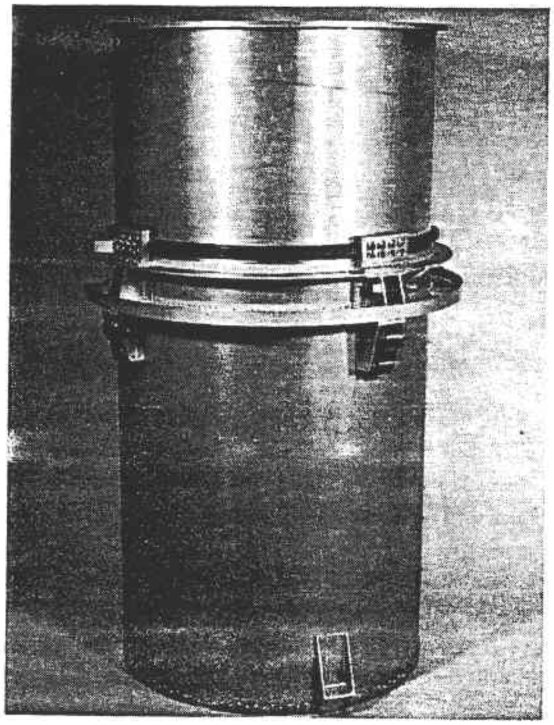

Stowage & Deployment Canister

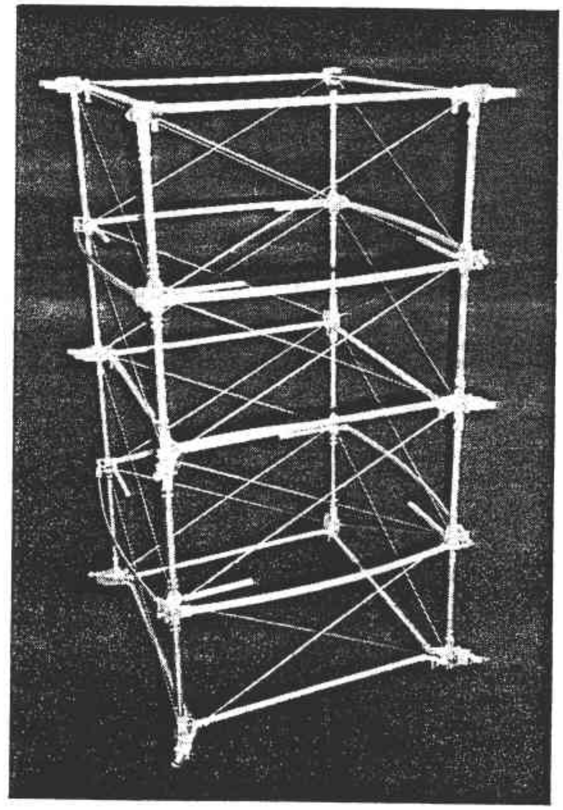

Deployed Mast

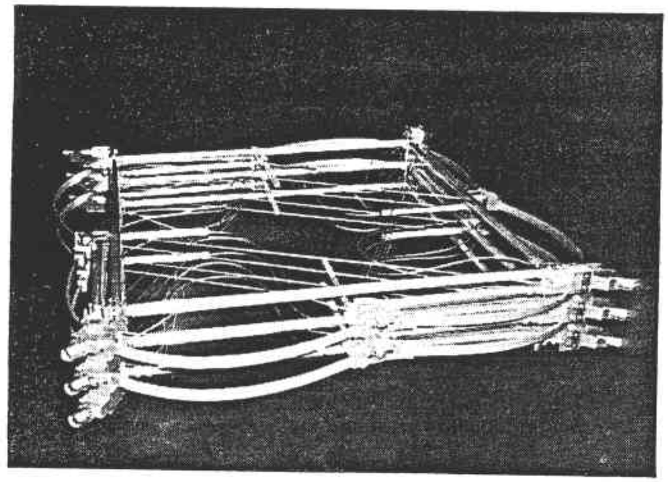

Stow Mast

Figure 5. Lattice Truss Stowage and Deployment

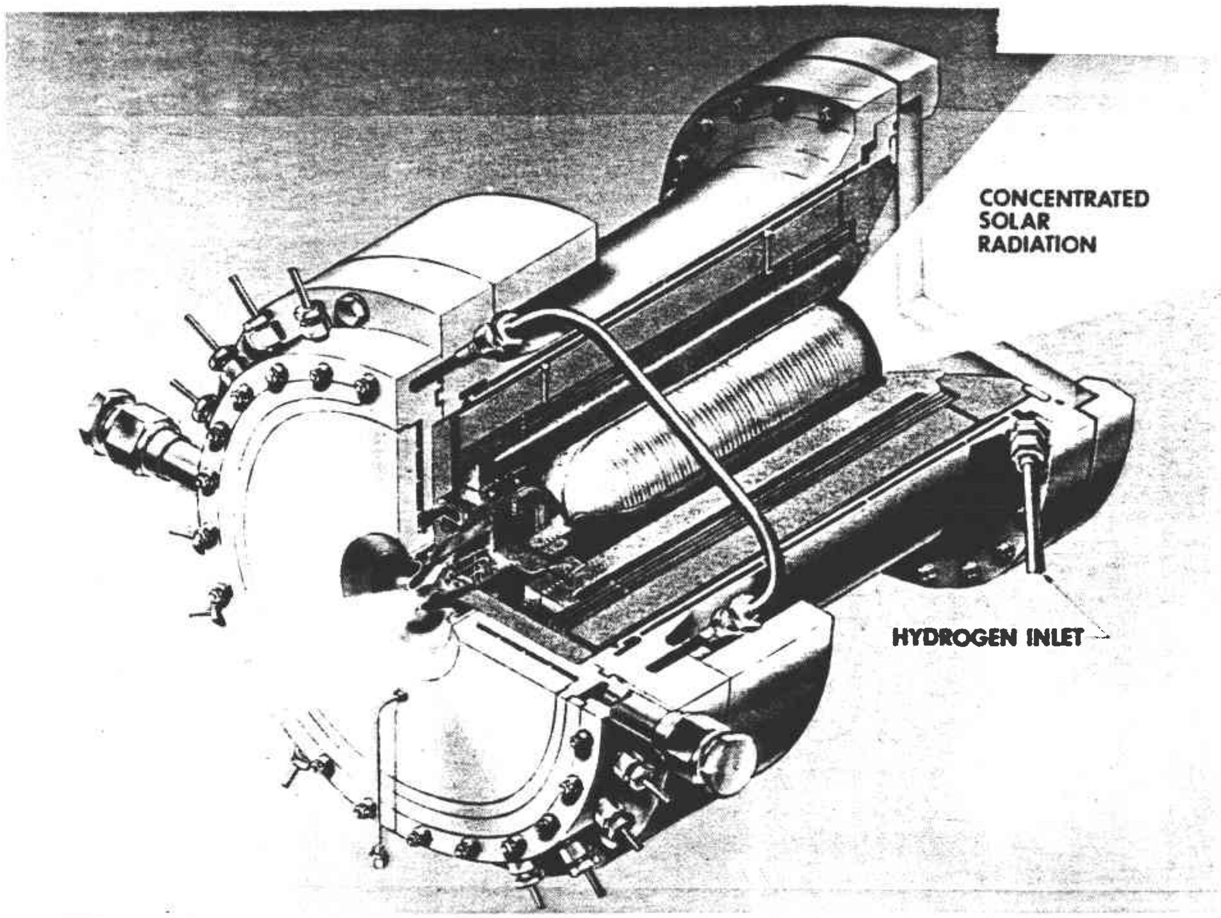

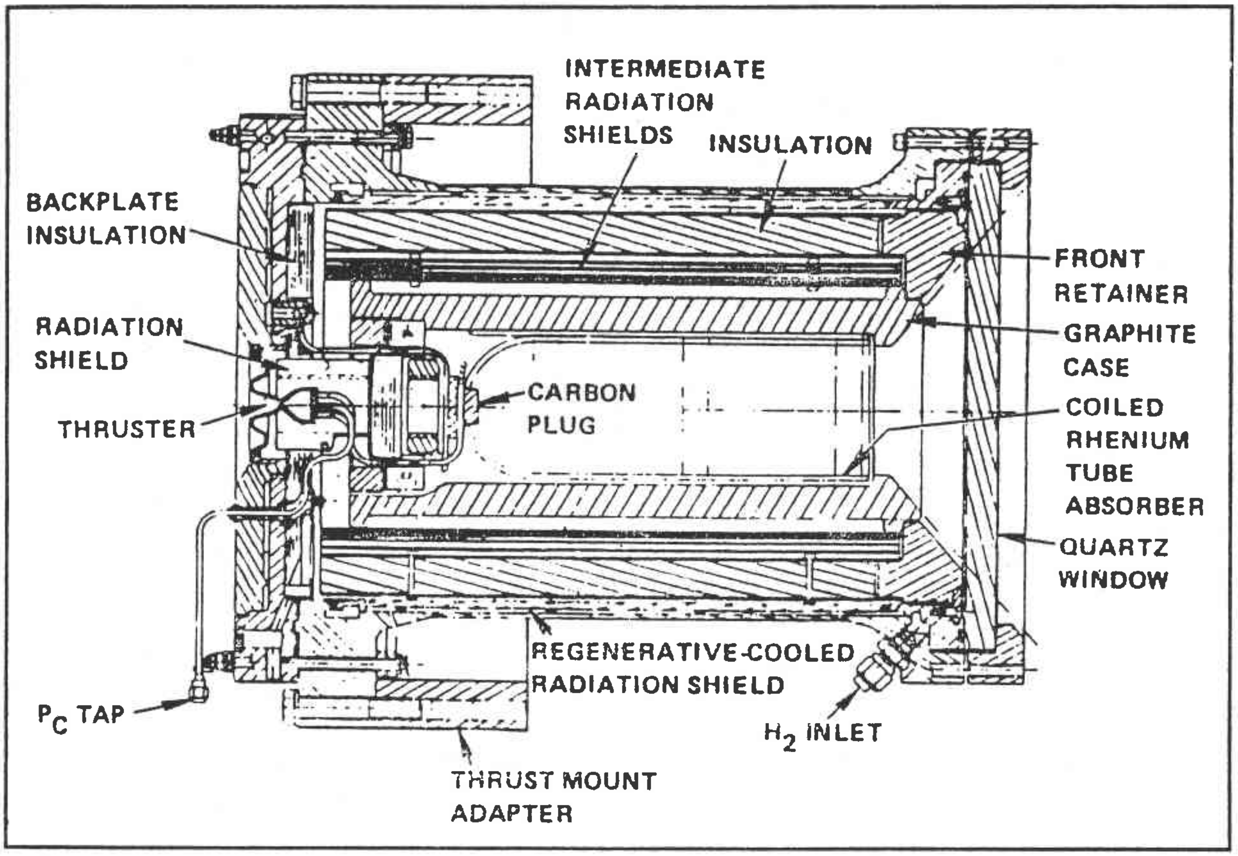

Figure 6. Solar Cavity/Thruster (References 3 and 10)

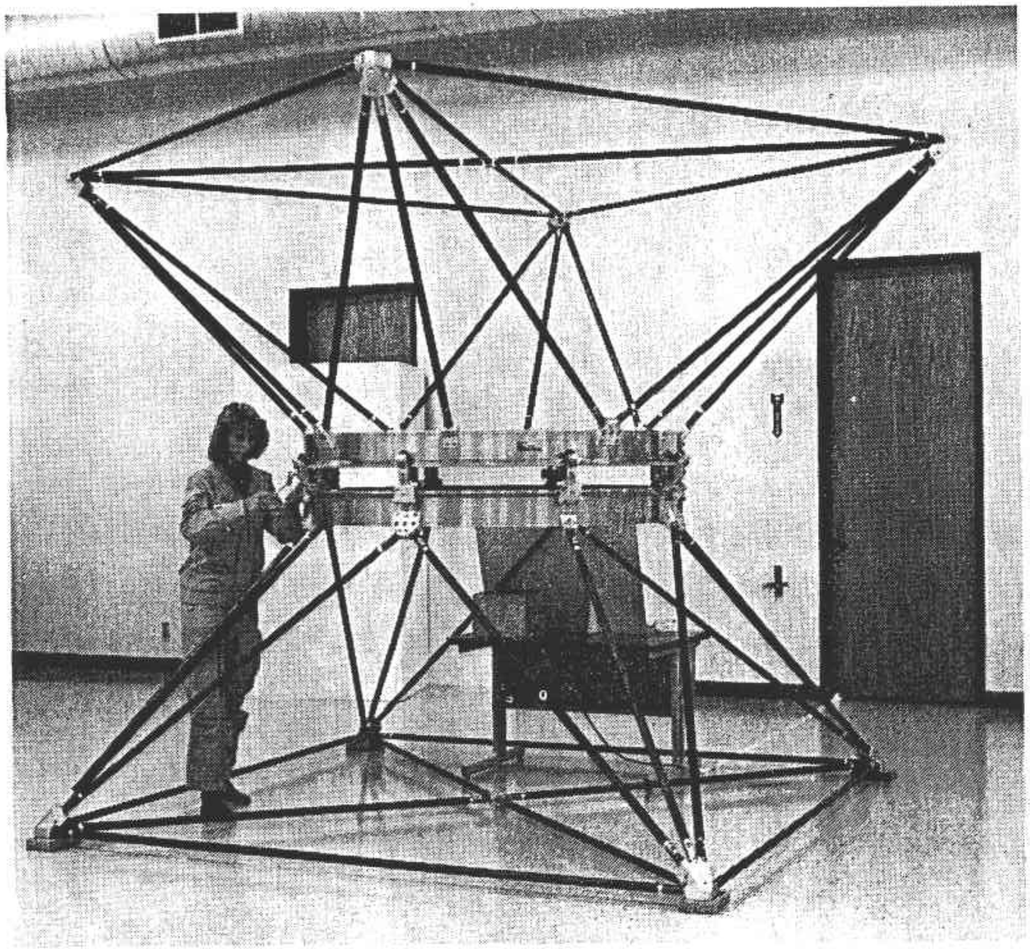

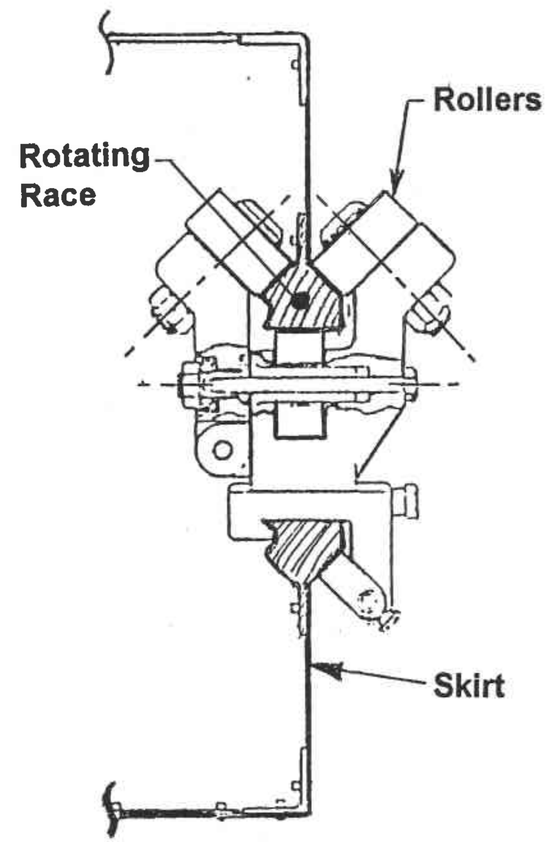

Figure 7. Space Station Alpha Joint Bearing (Reference 12)

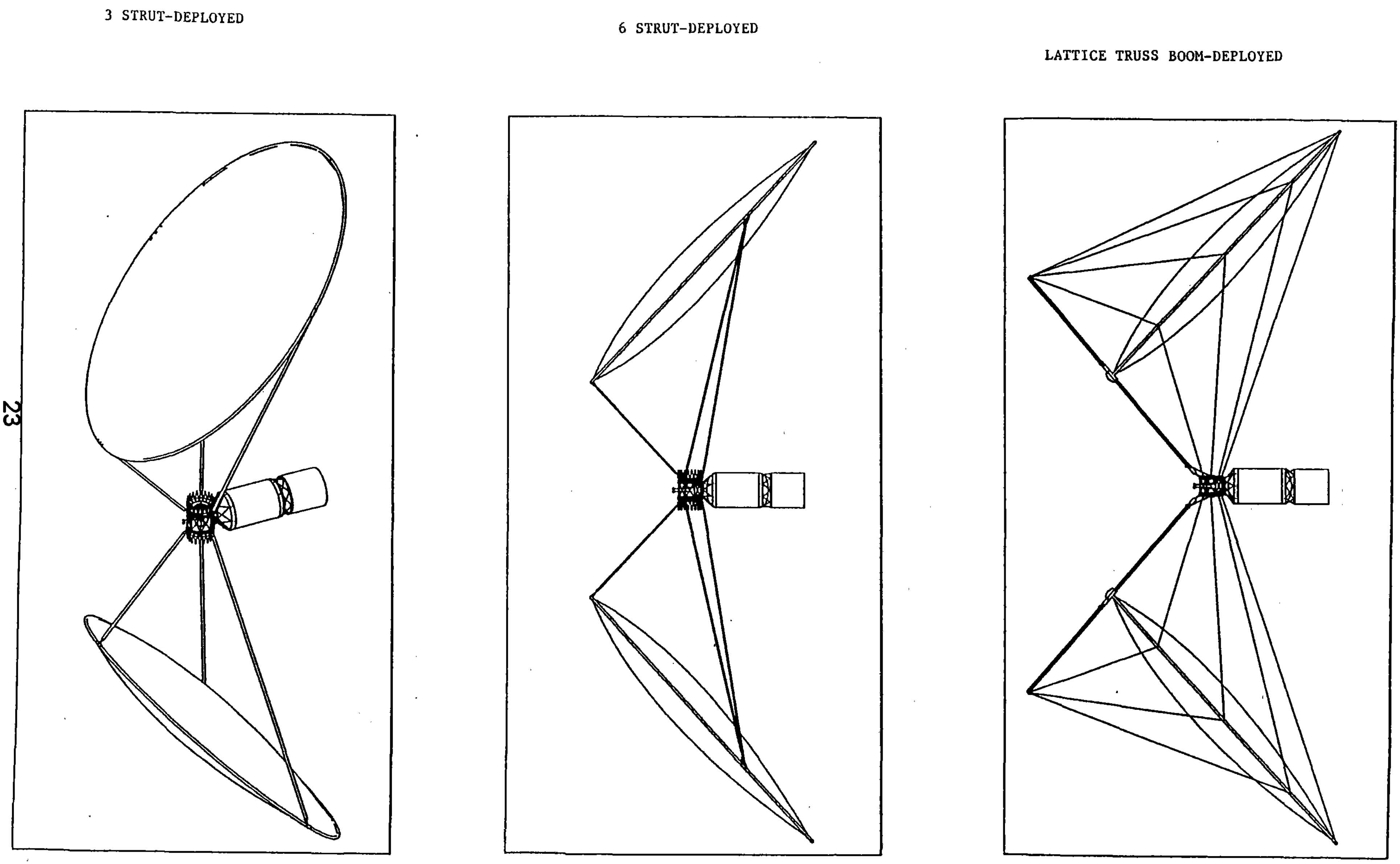

Figure 8. Solar Concentrator System Structural Concepts

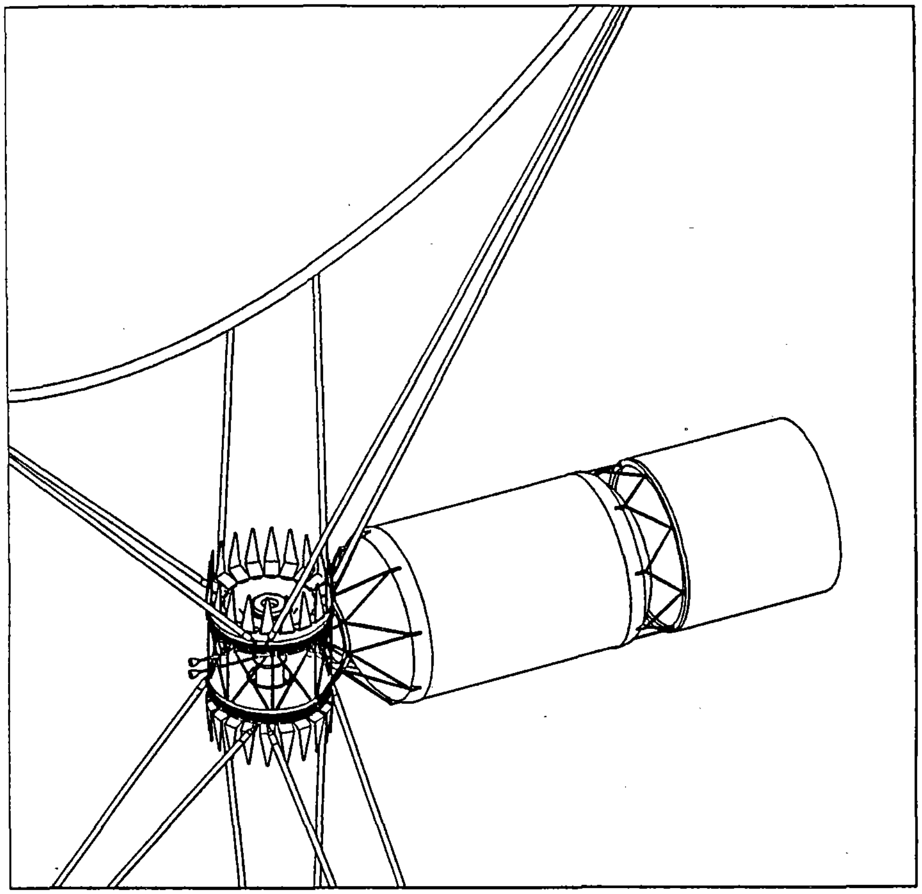

Figure 9. Six Inflatable/Rigidized Strut Concept

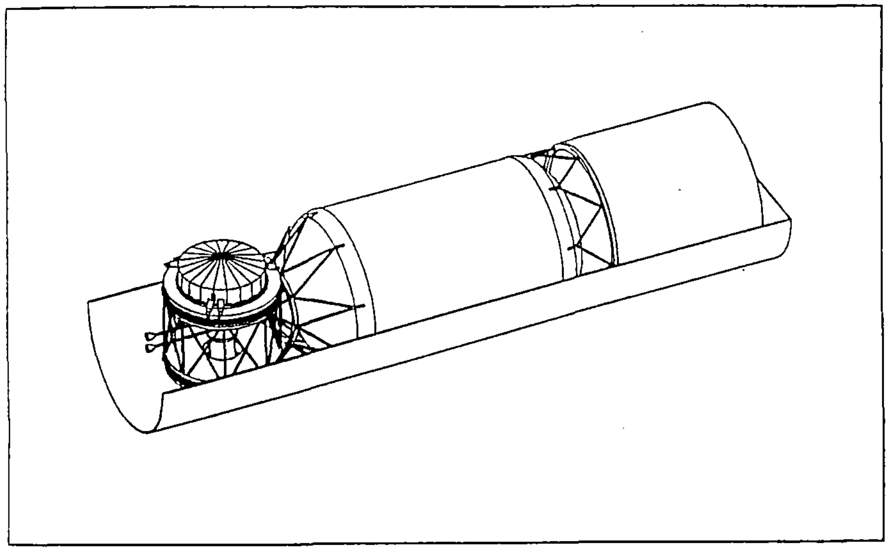

Figure 10. Stowed Configuration

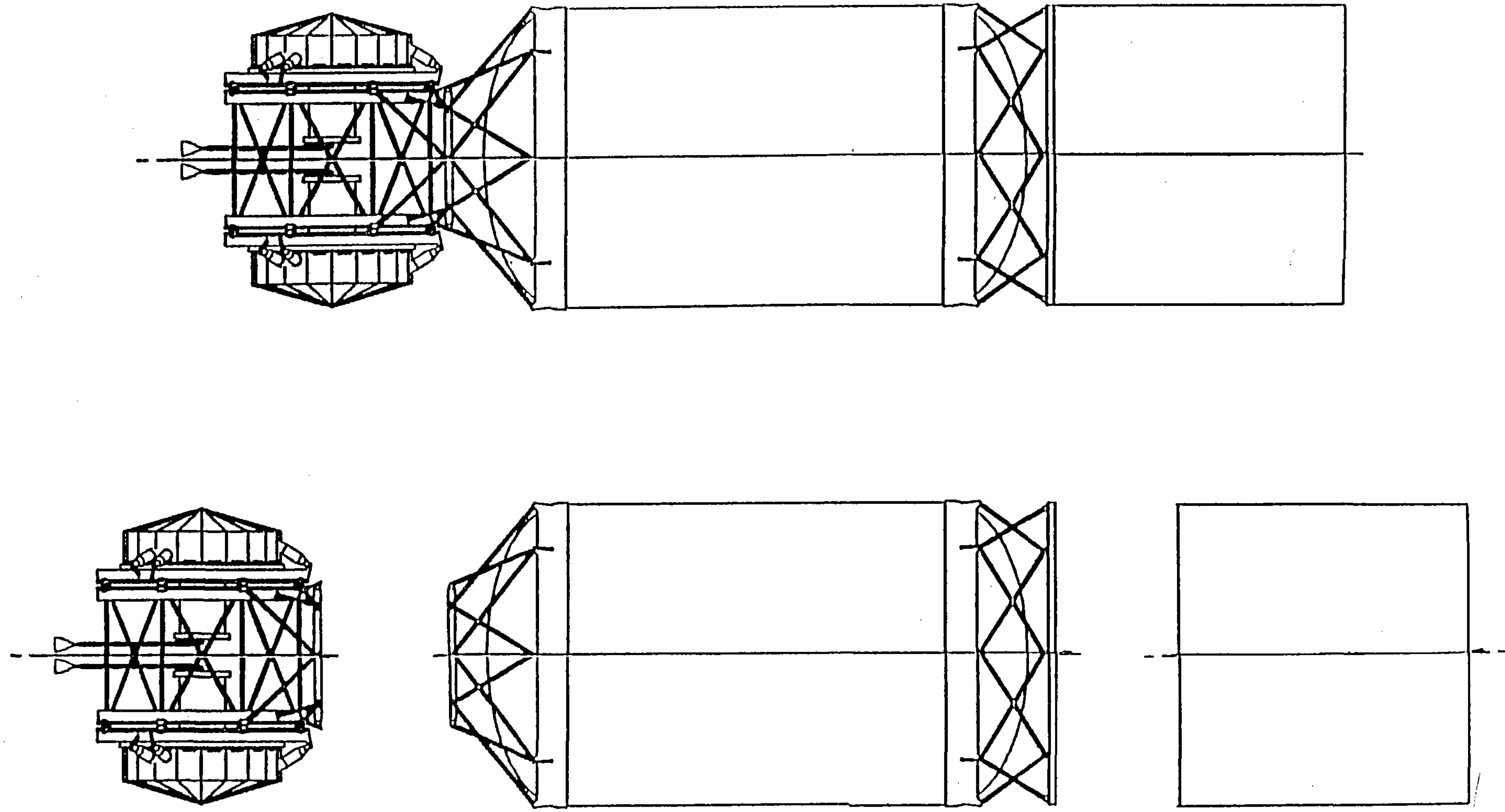

Figure 11. Solar Propulsion Vehicle Modularity

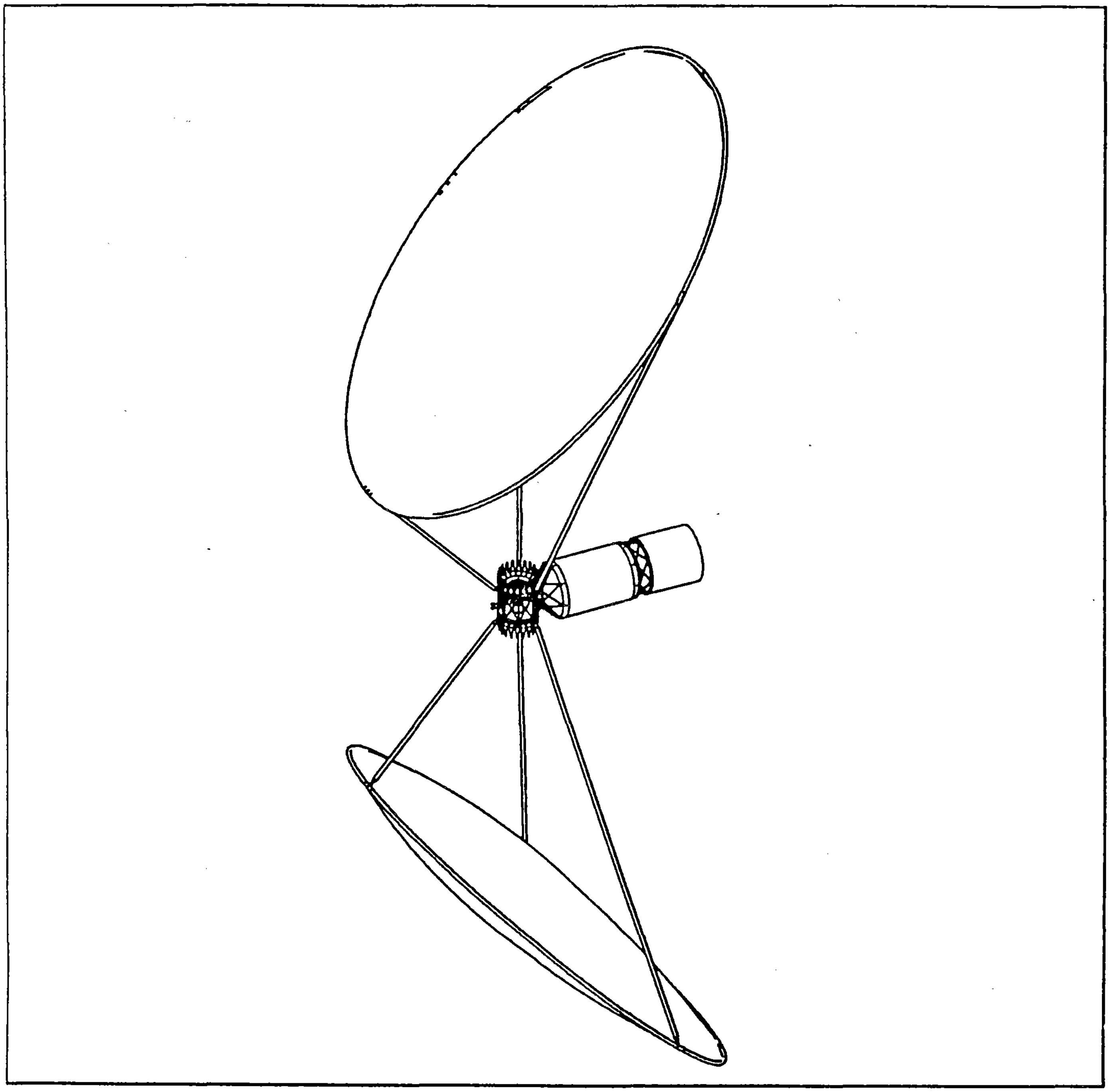

Figure 12. Three Inflatable/Rigidized Strut Concept

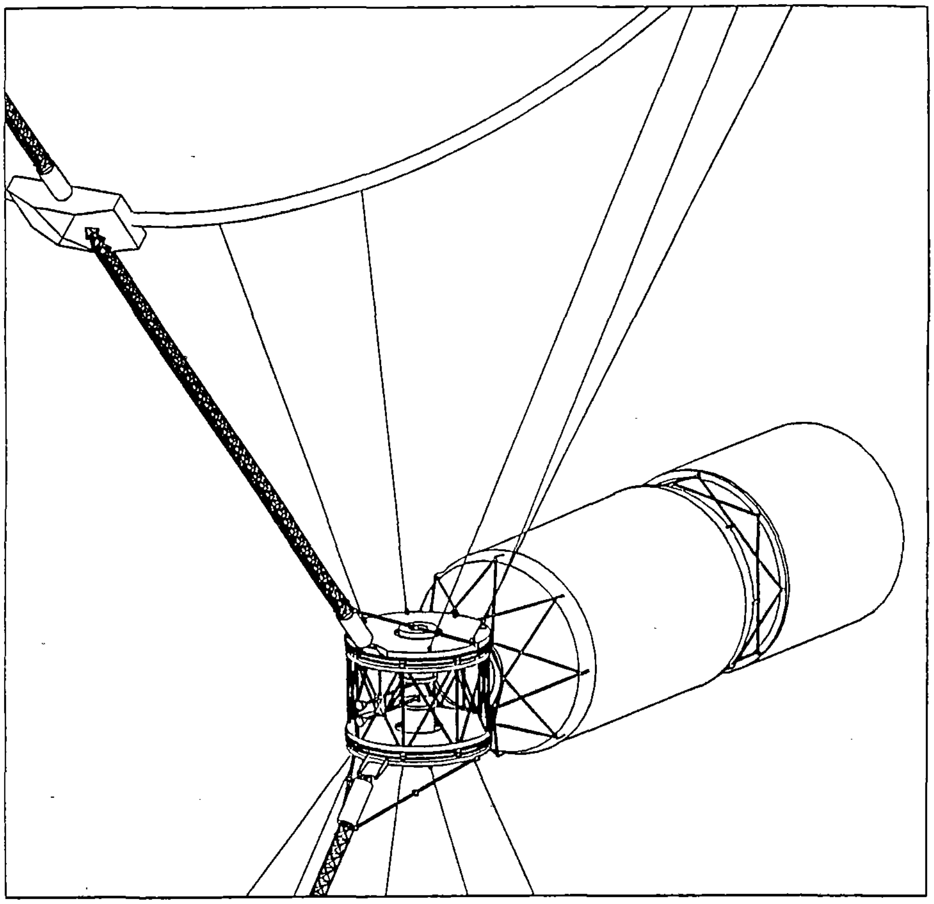

Figure 13. Deployed Lattice Truss Boom Concept

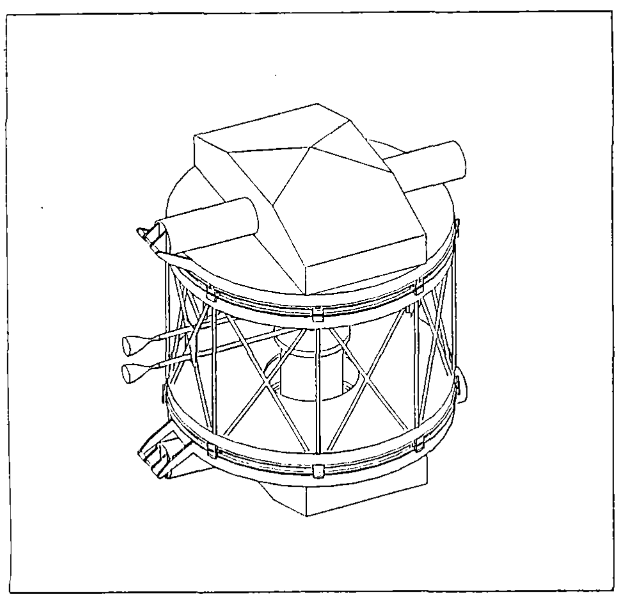

Figure 14. Stowed Lattice Truss Boom

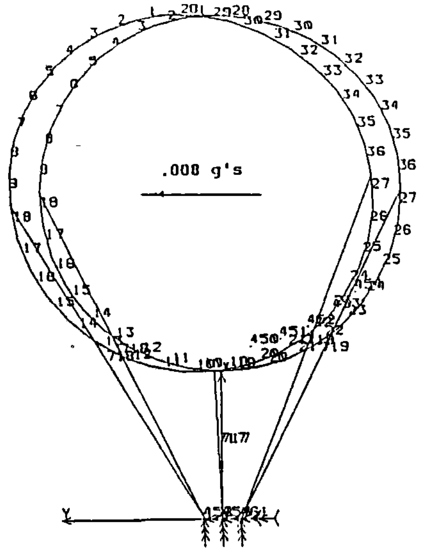

A. Three Strut

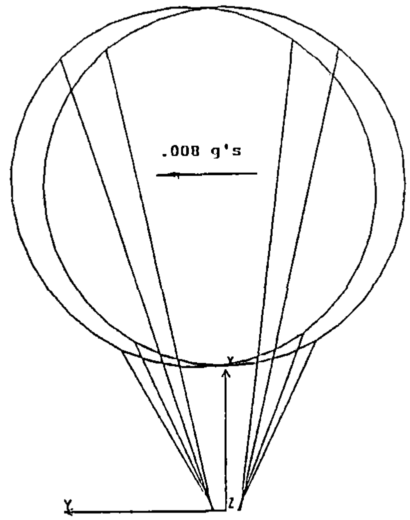

B. Four Strut

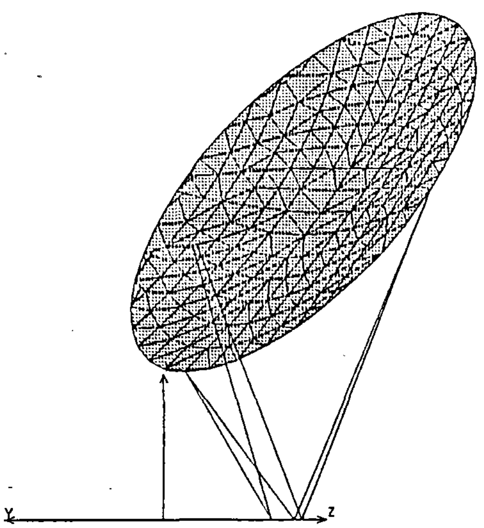

C. Six Strut Bipod

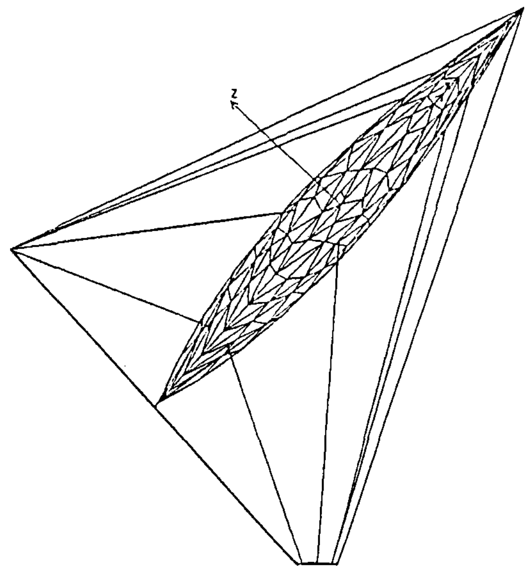

D. Lattice Truss Boom

Figure 15. Static Load Model Geometry

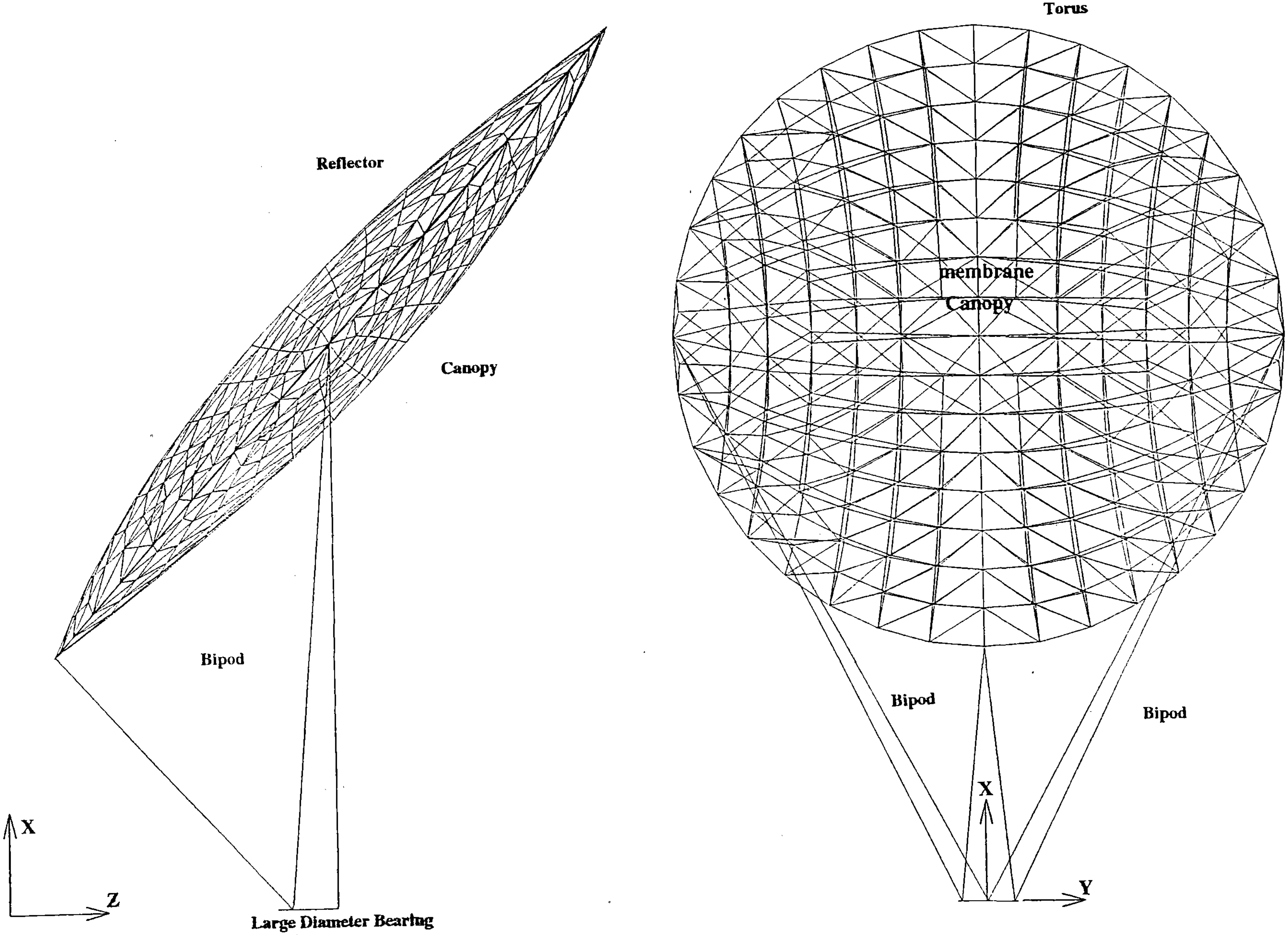

Figure 16. Structural Dynamic FEM Geometry

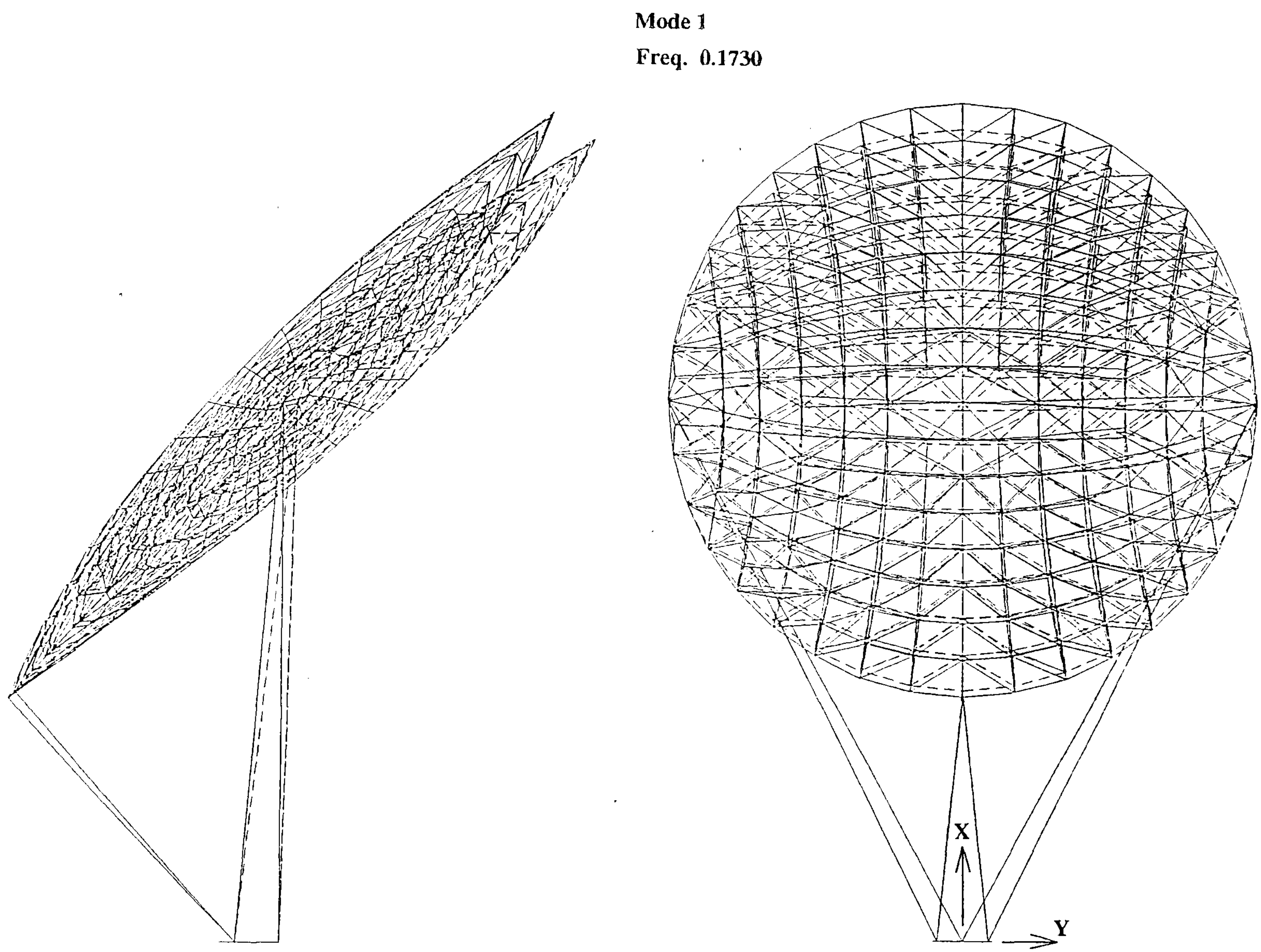

Figure 17. Mode 1 First Bending About Y-Axis

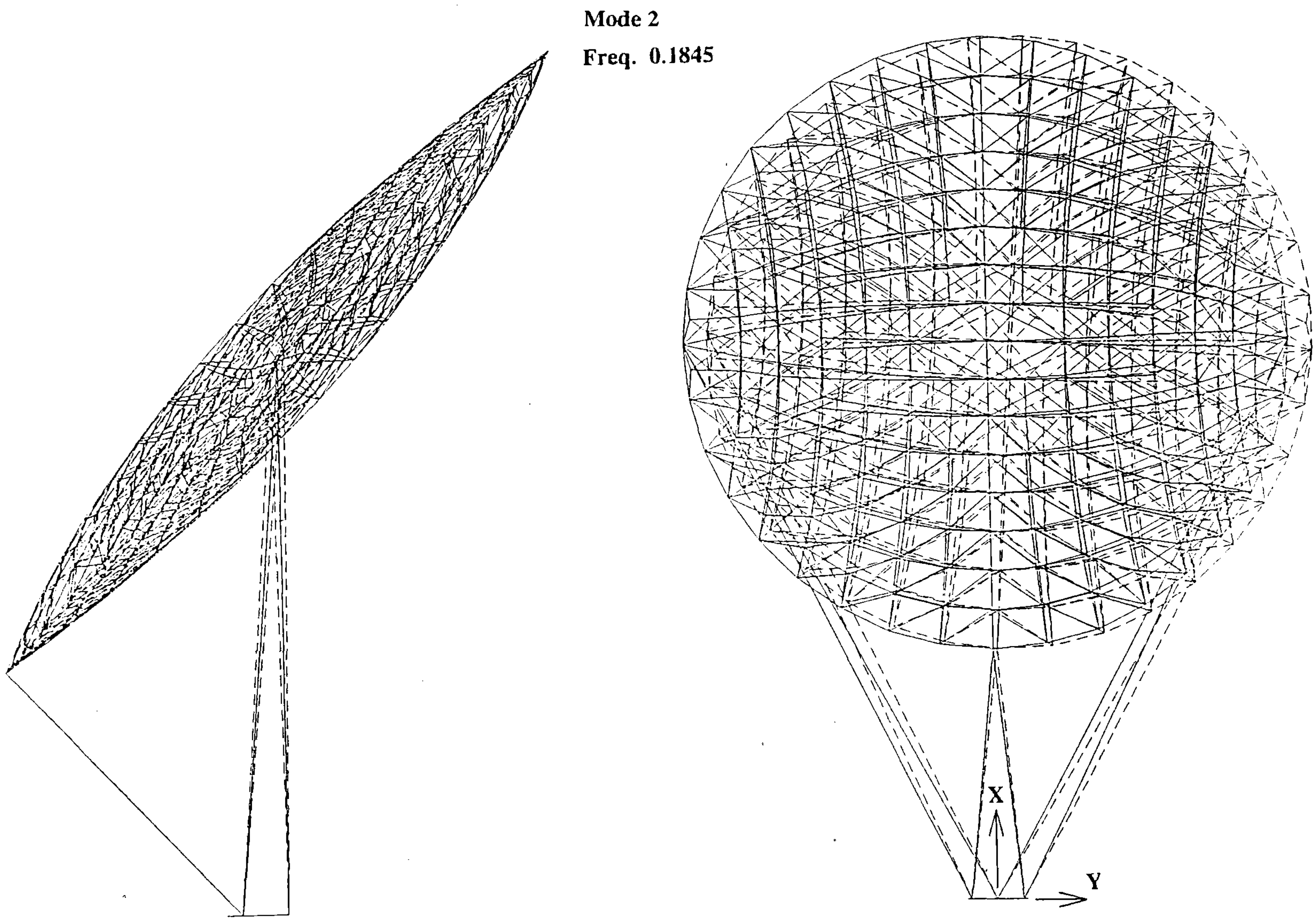

Figure 18. Mode 2 First Bending About Z-Axis

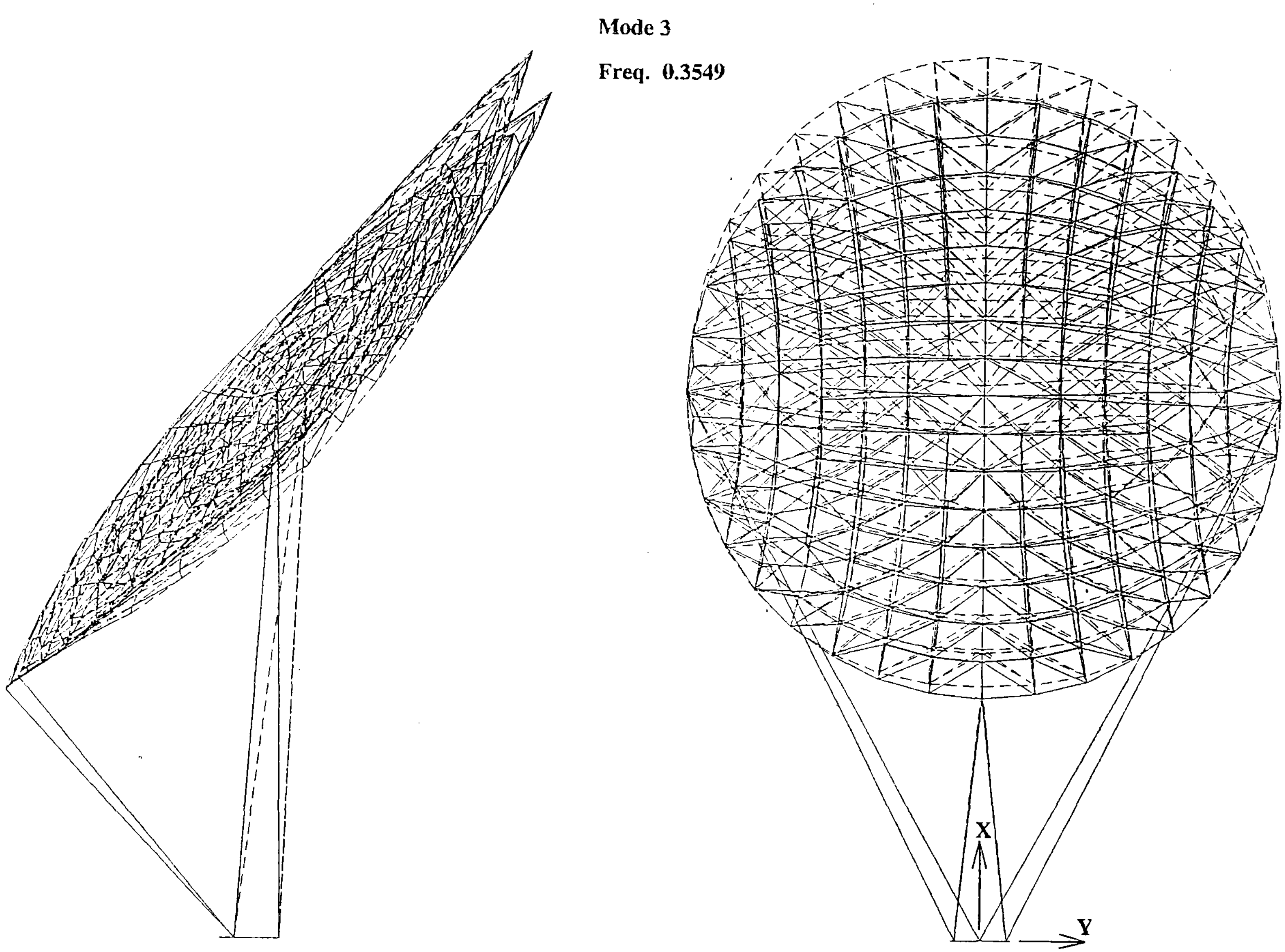

Figure 19. Mode 3 Second Bending About Y-Axis

Mode 4
Freq. 0.4335

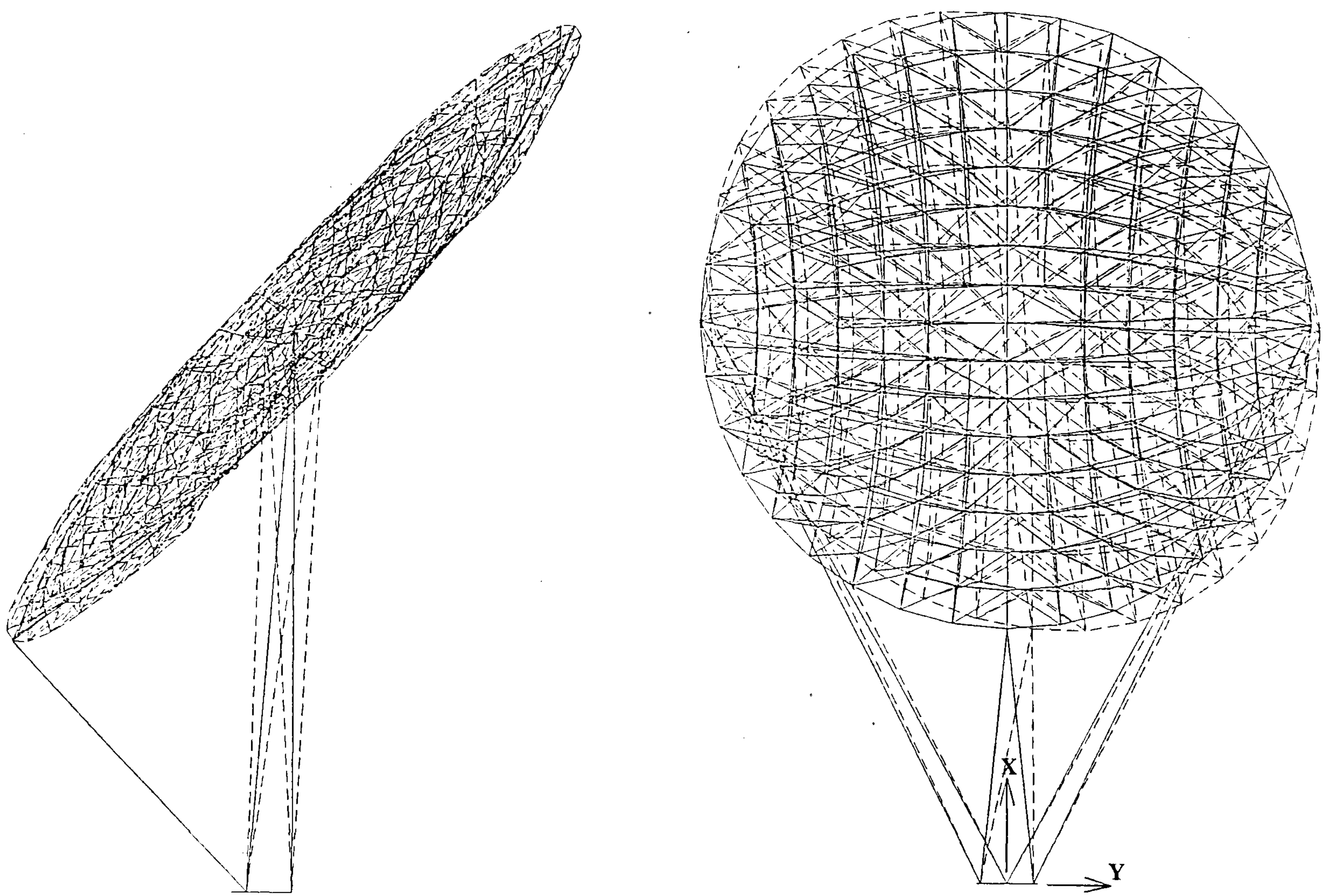

Figure 20. Mode 4 First Torsion About X-Axis

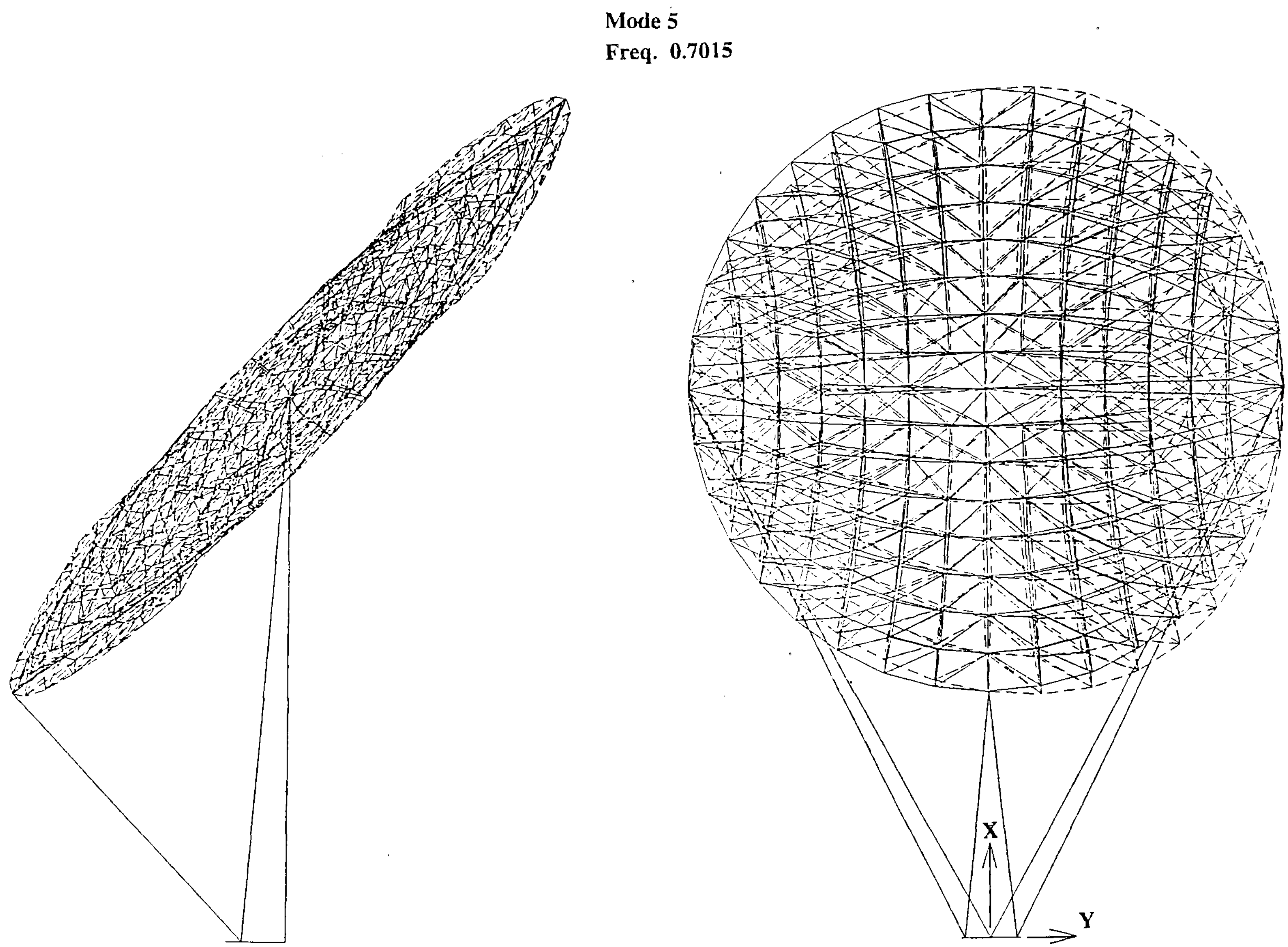

Figure 21. Mode 5 Torus Twisting About Minor Axis

Mode 6

Freq. 0.7212

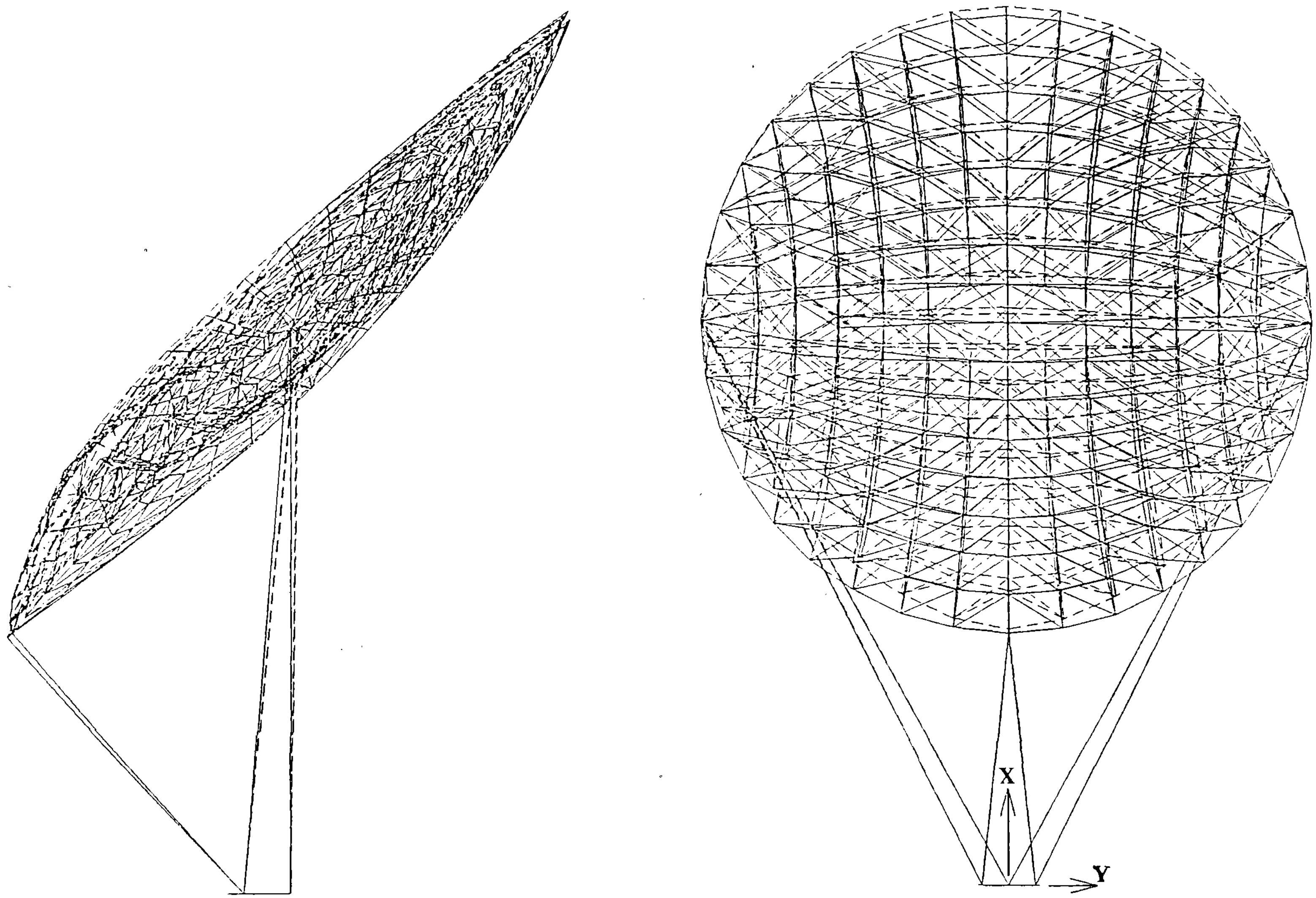

Figure 22. Mode 6 Torus Bending About Minor Axis

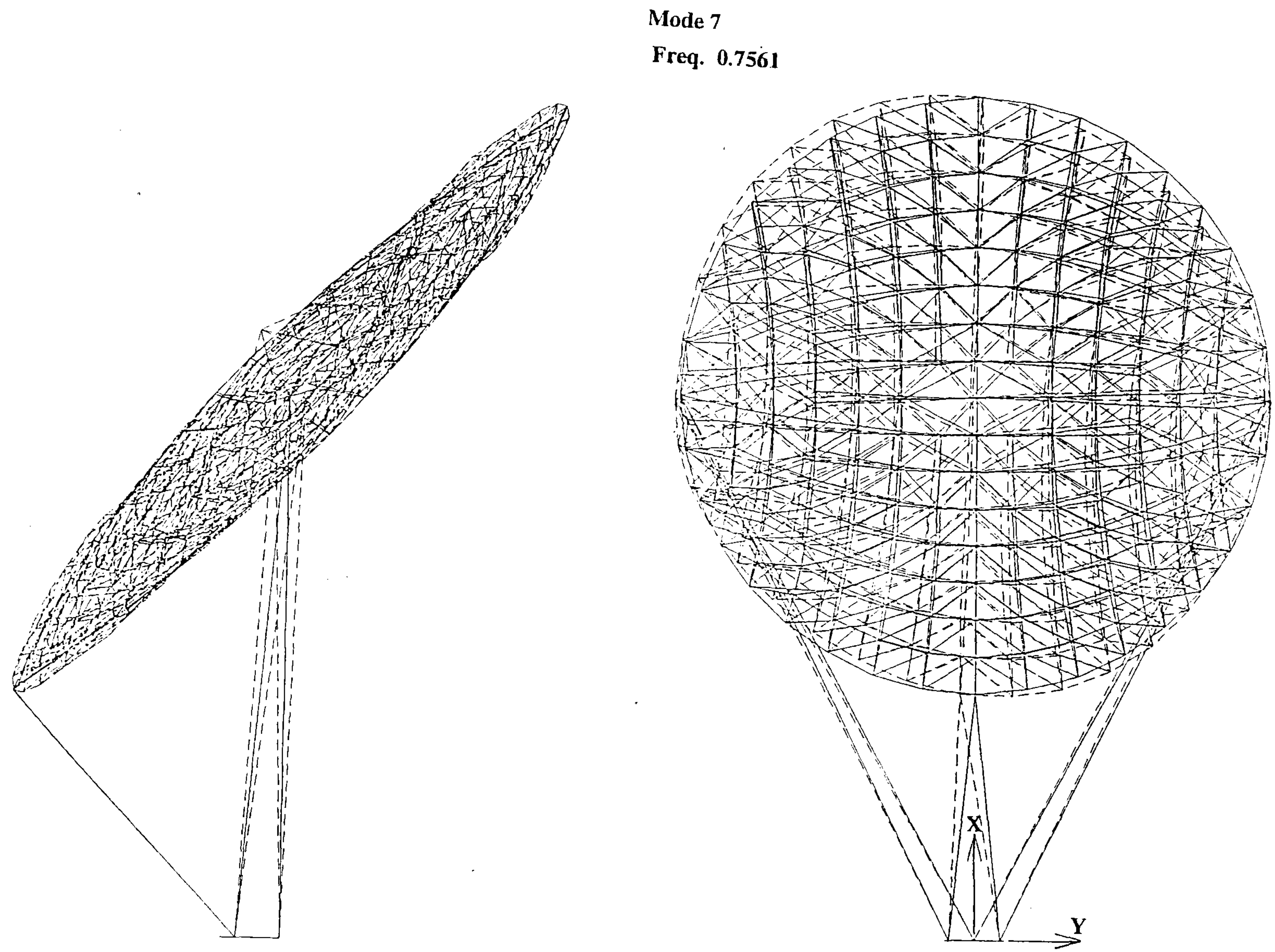

Figure 23. Mode 7 Second Torsion About X-Axis

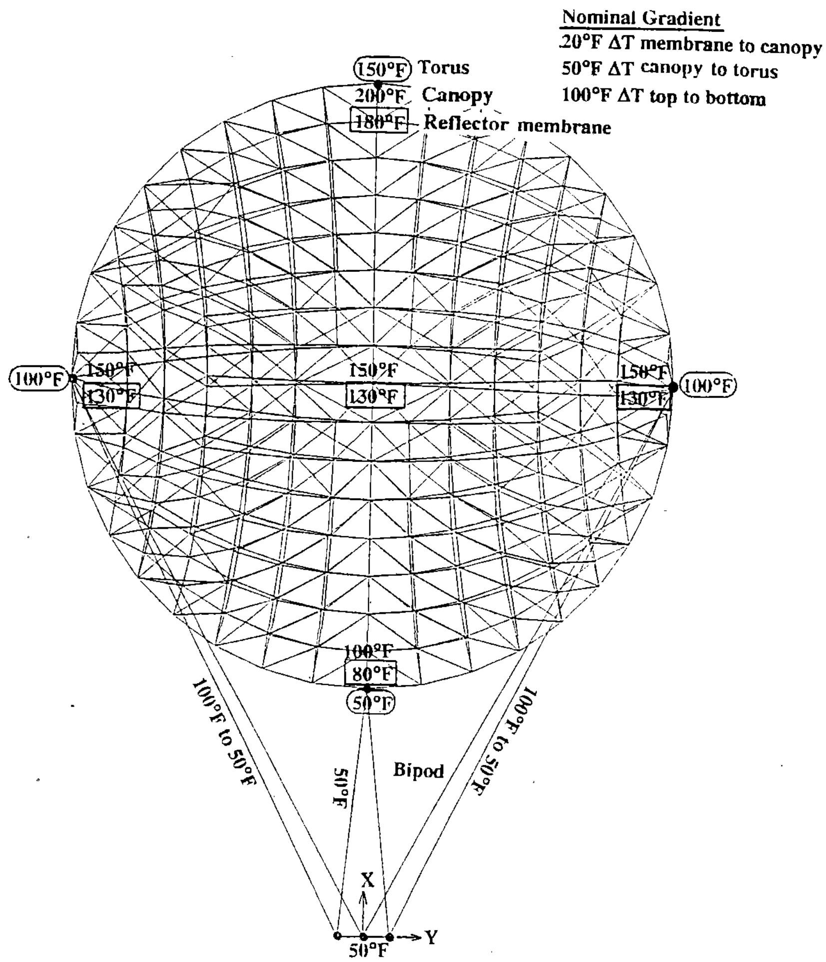

Figure 24. Thermal Distortion Temperature Profile

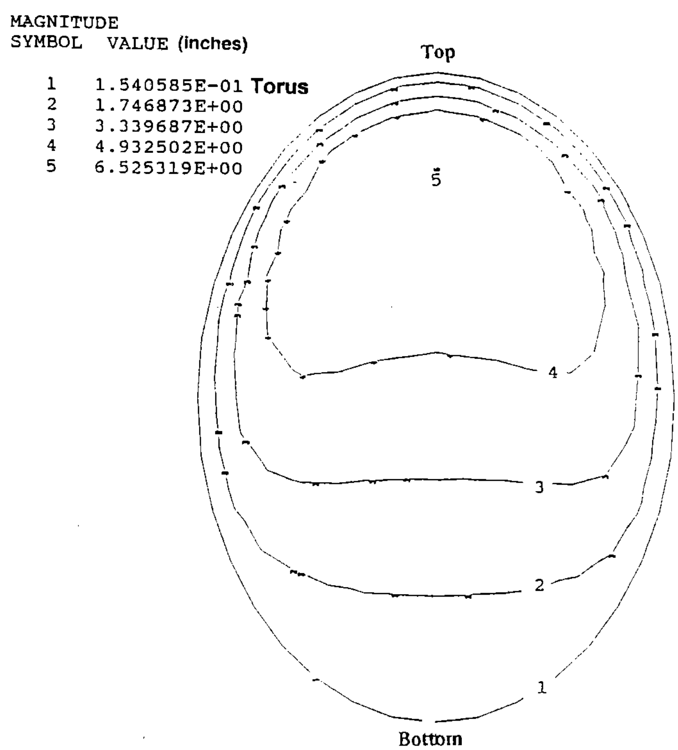

Figure 25. Concentrator Thermal Distortion Contour Plot

Table 1. Component Selections

Key component information for the solar propulsion system design has been obtained from the following source:

Component	Source	Reference No.
Concentrator/Torus	L'Garde, SRS, Contravas	4, 5, 7
Support Strut Concepts	L'Garde, SRS	4, 5
Solar Cavity/Thruster	Rockwell, Ultramet	3, 10, 11
Propellant Tank/Payload Size	Rockwell, Phillips Lab	1, 6
Gimbal Bearing System	AEC - Able	12
Deployable Lattice Truss	Astro, AEC - Able	8, 9

Table 2. Torus Displacement and Stress E = 100,000

RIM DISPLACEMENTS (INCHES) AS A FUNCTION OF RADIUS r

n	r (inches)				
	2	4	8	12	16
1	21200	2650	330	98	41
2	1190	150	19	5.5	2.3
3	181	23	3	0.8	0.4
4	49	6	0.76	0.23	0.10

APPLIED AND ALLOWABLE STRESSES

	n	r (inches)				
		2	4	8	12	16
σ_b psi	1	3274	819	205	91	51
σ_b psi	2	1054	264	66	29	17
σ_b psi	3	597	149	37	17	9
σ_b psi	4	322	81	20	9	5
σ_{MP} psi	--	2558	1270	640	426	320
σ_{CR} psi	--	348	141	54	29	19
w_T lbs	--	61	122	243	365	486

σ_b = Torus bending stress due to 0.008g

σ_{mp} = Torus compressive stress due to membrane inflation pressure 0.00025 psi

σ_{cr} = Allowable (critical) local buckling strength of torus

W_T = Torus weight lbs

Table 3. Torus Displacement and Stress

Three Point Support (n = 3) E = 500,000 psi

a. t = .02 inches

r (inches)	2	3	4	5	6
δ_{max}, inches	9.8	2.89	1.22	0.62	0.36
σ_b, psi	322	143	81	52	36
σ_{pm}, psi	2558	1705	1279	1023	853
σ_{cr}, psi	1743	1036	707	621	404
W_t, lbs	68	102	136	170	204

b. t = .03 inches

R (inches)	2	3	4	5	6
δ_{max}, inches	6.5	1.93	0.81	0.42	0.24
σ_b, psi	215	95	54	34	24
σ_{mp}, psi	1705	1136	853	682	568
σ_{cr}, psi	2880	1740	1210	900	710
W_t, lbs	102	153	204	254	305

c. t = .04 inches

r (inches)	2	3	4	5	6
δ_{max}, inches	4.87	1.44	0.61	0.31	0.18
σ_b, psi	161	72	40	26	18
σ_{mp}, psi	1279	853	640	512	426
σ_{cr}, psi	4068	2493	1743	1314	1036
W_t, lbs	136	204	271	339	407

Table 4. Structural Characteristics

COMPONENT	MATERIAL	E (psi)	t (inches)	DIAMETER (in.)	DENSITY (lb/in^3)
REFLECTOR	TEFLON	100,000	.00025	1200 x 1634	.050
REFLECTOR RIM	RIGIDIZED CLOTH	500,000	0.040	6.0	.050
COLUMNS	RIGIDIZED CLOTH	500,000	0.040	6, 8, 12	.050
GUY LINES	GRAPHITE	25E6	1/16 DIA		.060
BOOM 1	GRAPHITE	20E6	A = .330 in2	DIA = 36 EI = 8/3E0 GJ = 4.47E8	.060
BOOM 2 REINFORCED	GRAPHITE	20E6	A = .660 in2	DIA =36 EI = 1.49E10 GJ = 1.80E9	.060

Weight of the reflector and rim is 205 lbs.

Table 5. Static Load Analysis Results

Configuration	Total Weight (lbs)	Load Case	u_x	u_y	u_z	R_x	R_y	R_z
			Inches			Degrees		
3-8" tubes	362	L	.001	72.9	0.22	5.61	.005	3.33
		A	3.9	.06	59.4	.003	2.99	.005
3-12" tubes	440	L	.01	27	.06	2.09	.002	1.23
		A	1.62	.04	13.5	.002	1.12	.003
4-8" tubes	445	L	.009	68.8	.04	5.44	.001	3.06
		A	2.76	.03	56.5	.003	2.76	.001
2-8" tubes 2-12" tubes	528	L	.004	40.8	.05	2.83	.001	1.84
		A	2.04	.05	41.7	.001	1.12	.002
4-12" tubes	565	L	.01	27.0	.06	2.08	.002	.618
		A	1.64	.06	21.7	.007	1.12	.003
6-6" tubes	442	L	.001	1.61	.069	.124	.0002	.080
		A	.60	.138	1.78	.0001	.125	.0001
6-6" tubes(SS)	442	L	.43	1.65	.016	.127	.0002	--
		A	.32	.02	1.80	.0001	.127	--
Boom	270	L	.004	7.91	.002	.809	--	.354
		A	.036	.003	.111	.003	.005	.004
Reinforced Boom	346	L	.003	6.75	.0003	.690	.0002	.303
		A	.002	.001	.075	--	.0012	.0001

L = Lateral (y) direction
A = Axial (z) direction
(SS) Simple supported tube ends versus fixed ends in all other cases

Table 6. Material Properties

Item	Section Property	Modulus (msi)	CTE (μ in/in/F)	Weight (lb)
Reflector	0.00025" thick	E_x =0.1 E_y =0.1 μ_{xy}=0.3	50.0	19.5
Canopy	0.00025" thick	E_x =0.1 E_y =0.1 μ_{xy}=0.3	50.0	19.5
Torus	6"∅ x 0.04" thick	E_x =0.5 E_y =0.5 μ_{xy}=0.3	1.7	169.0
Bipod	6"∅ x 0.04" thick	E_x =0.5 E_y =0.5 μ_{xy}=0.3	1.7	236.0

Table 7. Bearing Stiffness

Stiffness	Component	120"∅ Bearing	64"∅ Bearing
Axial*	k_x	2.0×10^7 lb/in	1.0×10^7 lb/in
Shear	k_y k_z	7.5×10^4 lb/in 7.5×10^4 lb/in	2.5×10^4 lb/in 2.5×10^4 lb/in
Torsion	θ_x	2.0×10^9 in-lb/rad	8.5×10^8 in-lb/rad
Bending	θ_y θ_z	3.0×10^9 in-lb/rad 3.0×10^9 in-lb/rad	5.5×10^8 in-lb/rad 5.5×10^8 in-lb/rad

* Values based on $E \cong 13 \times 10^6$ psi
$t = 0.1"$
$l = 24"$
$r = 60"; 30"$

Table 8. Dynamic Analysis Results

No Preload in Torus

Mode No.	Frequency 120"∅ Bearing (Hz)	64"∅ Bearing (Hz)	Mode Description
1	0.1730	0.1728	1 st bending about y-axis
2	0.1845	0.1842	1 st bending about z-axis
3	0.3549	0.3547	2 nd bending about y-axis
4	0.4335	0.4297	1 st torsion about x-axis
5	0.7015	0.7015	torus twisting about minor axis
6	0.7212	0.7211	torus bending about minor axis
7	0.7561	0.7536	2 nd torsion about x-axis

Table 9. Dynamic Analysis Results

645 lbs Preload in Torus

Mode No.	64"∅ Bearing (Hz)	Mode Description
1	0.2441	1 st bending about y-axis
2	0.2607	1 st bending about z-axis
3	0.5001	2 nd bending about y-axis
4	0.6143	1 st torsion about x-axis
5	0.9894	torus twisting about minor axis
6	1.0130	torus bending about minor axis
7	1.0683	2 nd torsion about x-axis

Table 10. Thermal Distortion Analysis Results

	No Preload in Torus		645 lbs Preload in Torus	
Description	Transparent Canopy	Reflector	Canopy	Reflector
Max Principal	203 psi	141 psi	436 psi	84 psi
Min Principal	-439 psi	-391 psi	-541 psi	-489 psi
Max Shear	260 psi	210 psi	125 psi	98 psi
Displacement	14.2 in	15.4 in	6.2 in	6.5 in